MOTOR CONTROL DURING AMPHIBIOUS LOCOMOTION CHANGES MUSCLE FUNCTION IN *POlYPTERUS SENEGALUS*

LISHA LIANG

Thesis submitted to the University of Ottawa
in partial Fulfillment of the requirements for the
Master of Science degree in Biology.

Department of Biology
Faculty of Science
University of Ottawa

ABSTRACT

Polypterus is an extant fish that is used as a model to understand the fin-to-limb evolutionary transition. *Polypterus* exhibits muscle phenotypes relevant to this transition. In particular, plastic changes in bone and muscle in *Polypterus* have been shown in response to spending time in a terrestrial environment. Muscle fiber changes are usually associated with changes in the performance demand placed on those muscles. We hypothesize that muscle fibers are recruited differently between aquatic and terrestrial environments to explain the change in fiber type. How pectoral fin muscle activity changes between swimming and walking is mostly unknown. Hence, this study utilizes electromyography (EMG) and high-speed videography to understand how the muscle activity pattern and function of all four pectoral fin muscle groups change during swimming and walking in aquatically raised fish. In this experiment, aquatically raised fish were placed in water and on land to observe changes in fin muscle function between behaviours. This study aims to understand how the instantaneous changes in the behaviour of the fish, particularly in the pectoral fin, could explain the muscle plasticity found in previous research. This study showed that fish adduct their pectoral fins much faster with increased muscle effort during walking compared to swimming. The adductor muscle also had the biggest change in function, activating for the majority of the fin-stroke cycle and therefore undergoing eccentric contraction. The increase in muscle effort seen in this study is consistent with the muscle fiber transition seen in fish that spend long periods on land, and the dramatic change of EMG magnitudes found in the adductor muscle may explain muscle damage previously found following acute walking.

RÉSUMÉ

Le *Polypterus* est un poisson vivant qui est utilisé comme modèle pour comprendre la transition évolutive des nageoires aux membres. Le *Polypterus* présente des phénotypes musculaires pertinents pour cette transition. En particulier, des changements plastiques dans les os et les muscles du *Polypterus* ont été démontrés en réponse à une exposition prolongée à des environnements terrestres. Les modifications des fibres musculaires sont généralement associées à des changements dans la demande de performance imposée à ces muscles. Nous émettons l'hypothèse que les fibres musculaires sont recrutées différemment entre les environnements aquatiques et terrestres pour expliquer le changement de type de fibre. La façon dont l'activité musculaire de la nageoire pectorale change pendant la natation et la marche est en grande partie inconnue. Cette étude utilise donc l'électromyographie (EMG) et la vidéographie à haute vitesse pour comprendre comment le modèle d'activité musculaire et la fonction des quatre groupes des muscles de la nageoire pectorale changent pendant la natation et la marche chez les poissons élevés en milieu aquatique. Dans cette expérience, les poissons élevés en milieu aquatique ont été placés dans l'eau et sur terre ferme pour observer les changements de la fonction des muscles de la nageoire entre les comportements. Cette étude vise à comprendre comment les changements instantanés dans le comportement des poissons, notamment au niveau de la nageoire pectorale, pourraient expliquer la plasticité musculaire retrouvée dans les études précédentes. Cette étude a montré que les poissons adductent leurs nageoires pectorales beaucoup plus rapidement avec un effort musculaire accru pendant la marche par rapport à la natation. Le muscle adducteur a également connu le plus grand changement de fonction, s'activant pendant la majorité du cycle de marche et subissant donc une contraction excentrique. L'augmentation de l'effort musculaire observée dans cette étude est cohérente avec la transition des fibres musculaires observée chez les poissons qui passent de longues périodes sur la terre ferme, et le changement spectaculaire de l'amplitude de l'EMG trouvé dans le muscle adducteur peut expliquer les dommages musculaires trouvés auparavant après une marche aiguë.

ACKNOWLEDGEMENTS

First and foremost, I would like to sincerely thank my supervisor Dr. Emily Standen for bringing me into the amazing Standen lab and providing me the opportunity to closely study a fascinating amphibious fish. I am very thrilled to be the first person ever to explore the function of all pectoral muscles in both swimming and walking! I would like to take the chance here to show my appreciation to you. I am very grateful to have a cheerful, passionate, and inspiring supervisor like you. Thank you very much for igniting my passion for biomechanics and doing everything you can to keep me motivated and encouraged the past two years. I always enjoy the weekly meetings with you, which have guided and supported me throughout the program. Everything that you have taught me had a profound impact on my research and professional skills, and made me a better researcher. Without you, I would never have made it this far in the journey.

Dr Roslyn Dakin and Dr Jean-Michel Weber, it has been such an honor to have you in my thesis committee. Thank you for providing wonderful feedback on my research, which helped me to think out of the box and improve my thesis story. Thank you for helping me throughout my master's program with your expertise.

Thank you, Keegan Lutek, for helping with my experiments and providing critical feedback on my work. I appreciate the time you took to discuss my project with me and your patience when I was facing difficulties. I enjoyed our discussions which helped me learn and inspired fascinating ideas to strengthen my thesis story. Your support through the discussions about and edits to my writing have helped keep me productive and guided me to think critically about my study. I cannot be more thankful for all your help in building up this research!

Special thanks to Trina Du, Gurjit Bhamra, Jeffrey Hainer, Cassandra Donatelli, and everyone in the Standen Lab for being supportive as I met roadblocks when setting up my experiment and running data analysis. Thank you all for providing me with advice and being supportive during the research.

Thanks to Ephraim and all my friends for all the mental support in the past two years, and special thanks to Yefei Zhou for helping in picking the colour palette for the plots. Thanks to my roommate Zhou Zhou Shu for your high-pitched voice which kept me awake at work.

Last but not least, I need to thank my family for their unconditional love and caring. Thank you for supporting me throughout those two years in every aspect. Mom and dad, thank you for understanding and letting me work on the things I am passionate for. Thank you for comforting me and making me believe in myself during the stressful moments in my research. I appreciate the interpersonal skills you taught and the little tricks on time management to help me reach my goals. I would like to thank my big brother for clearing out my negative thoughts when I had anxieties. You can be harsh and critical sometimes, but all the advice you have given me pushed me further and helped me to be successful. You are the best brother in the world.

TABLE OF CONTENTS

LIST OF TABLES

LIST OF FIGURES

LIST OF ABBREVIATIONS

abd. pro. – abductor profundus

abd. sup. – abductor superficialis

add. – adductor

ANOVA – analysis of variance

ATP – adenosine triphosphate

CIs – confidence intervals

cl – cleithrum

coraco – coracometapterygialis

d.f. – degrees of freedom

EMG – electromyography

emmean – estimated marginal mean

FLC – force-length curve

fps – frames per second

FVC – force-velocity curve

LME – linear mixed effects model

lp – lepidotrichia

ms – mesopterygiuml

MS-222 – tricaine methanesulfonate

mt – coracometapterygialis

mt – metapterygium

P. senegalus – *Polypterus senegalus*

pr – propterygium

rd – radials

RIA – rectified integrated area

s.e.m. – standard error of the mean

sc – scapulocoracoid

THRIA – time to reach half the rectified integrated area

zono – zonopropterygialis

Chapter 1: Broad Introduction

1.1 Background Information: Origin of tetrapods and *Polypterus*

Hundreds of millions of years ago, the evolution of vertebrates saw our ancestors move from water onto land with the advent of tetrapods and a pivotal fin-to-limb transition (Clack, 2012). However, late Devonian extinctions resulted in massive loss of marine species in fossil records and left a gap in our knowledge of the transition of primitive fish to stem tetrapods (McGhee, 2013). The mechanisms of anatomical, functional, and physiological pectoral fin adaption to the terrestrial environment during the fin to limb transition is still being studied. To help us understand how primitive fish could have used their fins to walk, we need an extant amphibious fish that shares comparable morphologies with the stem tetrapods. *Polypterus senegalus* is one of the most basal extant actinopterygians, which shares a common ancestor with early tetrapods. Two other extant fishes that are closely related to tetrapods phylogenetically, are coelacanths and lungfish. Both coelacanth and *Polypterus* have six muscles across the shoulder joint, but the coelacanth does not have all the muscles originating from the pectoral girdle and wrapping around the glenoid like *Polypterus*. Although coelacanth has additional muscles within the pectoral girdle with higher complexity than *Polypterus* (Miyake et al., 2016), coelacanths live in deep-sea environments which makes them difficult to study. Lungfish have paired lungs like *Polypterus*, however, the most common lungfish have pectoral and pelvic fins that are too slim to support terrestrial locomotion. The second genus of lungfish (*Neoceratodus*) does have lobed pectoral fins with a relatively simple muscle structure consisting only of the adductor and abductor muscles. Although these muscles originate from the pectoral girdle in both fish and tetrapods, they do not cross the glenoid in fish (Wilhelm et al., 2015), limiting their functional similarity to tetrapod muscles. Although, because of its phylogenetic position, *Neoceratodus* would make an interesting model, it is an endangered species which makes it a poor choice for studying fin use on land.

Polypterus is a primarily aquatic fish, that has lobed pectoral fins which can be used for walking overland (Standen et al., 2016), and paired lungs (Graham et al., 2014), which allow them to breathe air. Moreover, *Polypterus* are easily accessible through the pet trade and have a complex pectoral musculature that appears intermediate between fish and tetrapods (Wilhelm *et al.*, 2015). *Polypterus* has robust and complex pectoral fin muscle architecture and skeletal structure which helps support their body when walking on land (Standen et al., 2016). In addition, *Polypterus* has been used in various studies where they have been held for extended periods on land (Du & Standen, 2017; Standen et al., 2014). This change in environment resulted in strengthening and elongation of the pectoral girdle bones similar to what is seen in the fossil record (Standen et al., 2014), and a change in pectoral fin muscle fiber type from aerobic to glycolytic (Du & Standen, 2017). In addition, it appears that significant damage occurs in particular pectoral fin muscles after short bouts of walking. The goal of this project is to understand how *Polypterus* pectoral fin muscle activation patterns change between walking and swimming to understand the mechanism that drives short-term tissue damage and longer-term muscle plasticity seen in previous studies.

1.2 Musculoskeletal structure of the *Polypterus* pectoral fin

In *Polypterus*, the pectoral girdle is located behind the head and articulates with the pectoral fins. Each side of the girdle has a socket-like structure consisting of a scapula and coracoid, which form an inverted glenoid fossa that articulates with the basal components of the pectoral fin (pro and metapterygia), as in **Figure 1.1**. Proximal to the fish head, two bones protrude from the scapulocoracoid: a long bone, the propterygium, and a short bone, the metapterygium. Moving distally, both bones expand laterally, leaving room for the mesopterygial plate in between. They articulate with small bony elements (medial radials) which eventually lead to rod-like radials. The arrangement of proximal longer and shorter bones (propterygium and metapterygium) and distal digit bones (radials) shows a similarity to zeugopod and autopod in tetrapods (Schneider & Shubin, 2013), and the radials of *Polypterus* seem to be a homologous equivalent to the metacarpals of autopod in tetrapods (Cuervo et al., 2012). The similarity of *Polypterus* fin skeletal structure with that of tetrapods could provide higher flexibility in movement and make it more prone to walk on land compared to other fishes.

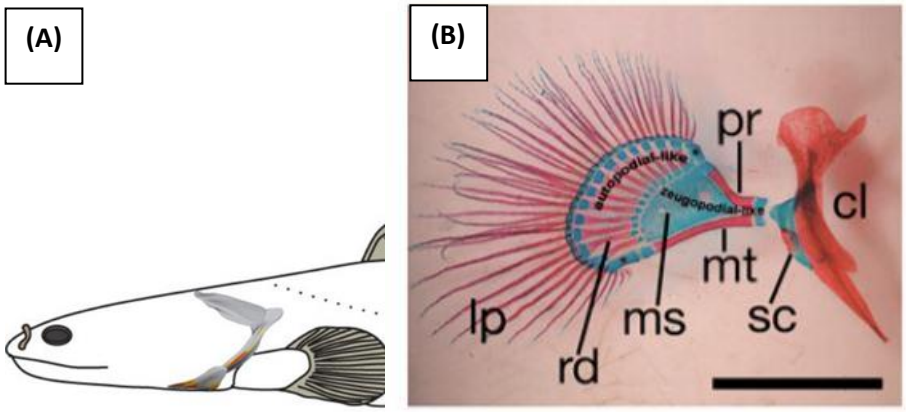

Figure 1.1: Pectoral fin structure in Polyterus senagalus. (A) shows the lateral view of the left pectoral girdle on an illustrated Polypterus (picture borrowed from Standen et. al., 2014). (B) is a frontal view of the right pectoral fin muscles and skeleton with scale bar = 5 mm. (Picture borrowed from Cuervo et al., 2012). The main musculoskeletal structures of the pectoral fin are shown in (B) as: cl,cleithrum; sc, scapulocoracoid; mt, coracometapterygialis; ms, mesopterygium; mt, metapterygium; pr, propterygium; rd, radials; and lp, lepidotrichiaSuperimposed on the pectoral girdle, there are six independent muscles (**Figure 1.2**): abductor superficialis (abd. sup.), abductor profundus (abd. pro.), adductor (add.), zonopropterygialis (zono), and coracometapterygialis (coraco) I and II.

The fin muscles originate entirely on the pectoral girdle, wrapping around the glenoid, and inserting distally within the fin. As shown in **Figure 1.2**, the abductor runs along the lateral side of the pectoral fin, and it is composed of abd. sup. and abd. pro. The abd. sup. has an extended origination that covers both scapulocoracoid and the lower cleithrum. It runs across the proximal abd. pro. and inserts into the propterygium (Wilhelm *et al.*, 2015). The abd. pro. originates laterally and ventrally on the scapulocoracoid. It inserts broadly on the distal pectoral fin skeleton

including the fin rays. Based on the anatomical position, the abd. pro. appears to be responsible for abduction and abd. sup. would act for pronation when abducting the fin. Opposed to the abductor muscles, the adductor originates from the distal scapulocoracoid running across the entire medial side of the fin into the distal bones and fin rays. In addition, the adductor has two distinct origin heads: one at the dorso-medial side and one at the medial side of the scapulocoracoid; but the muscle is defined as one muscle. The two origin heads intermix when moving down towards the end/proximal side of the fin, and therefore, make them indistinguishable as two subdivions (Wilhelm *et al.*, 2015). The adductor appears to help with pronating and adducting the pectoral fin. On the ventral side, both coraco I and II originate from the lower scapulocoracoid and insert on the metapterygium. Both muscles act to depress and supinate the pectoral fin. On the dorsal side, the zono originates from the medial cleithrum and upper scapulocoracoid and inserts on the proximal propterygium. The zono elevates the pectoral fin and may also supinate and pronate the fin (Wilhelm *et al.*, 2015). The abundance of clearly differentiated muscles across the glenoid joint potentially increases fin behavioural flexibility, particularly in rotation, so that the fish could have more control of the pectoral fins in response to a novel terrestrial environment.

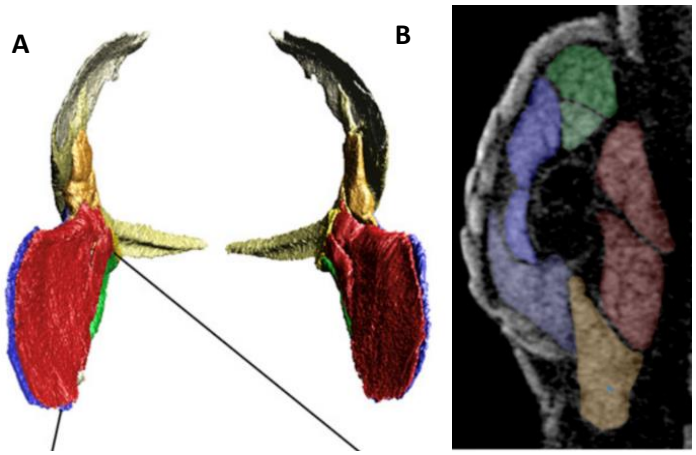

Figure 1.2: MicroCT scan of contrast-enhanced stained muscle arrangement in pectoral fin muscle of *P. senegalus* (Wilhelm et al., 2015). (A) is a posterior view of the two pectoral fins with pectoral gridles (the white curvy bone structure) attached. (B) is a cross-section view of the left pectoral fin muscle including the six independent muscles, which are coraco I and II (in green), abd. pro. and aubd. sup. (in blue), zono (in yellow), adductor (in red)

1.3 Walking and Swimming Biomechanics in *Polypterus*

As an amphibious fish, *Polypterus* is not only capable of aquatic locomotion but is also able to perform terrestrial excursions on land (Du et al., 2016). *Polypterus* have highly distinct locomotion in swimming versus walking as demonstrated in **Figure 1.3**. In water, *Polypterus* mainly relies on synchronized pectoral fin oscillation for generating thrust (as a labriform swimmer) while the body remains straight with slight tail oscillations that appear more force stabilizing than thrust producing. Whereas, on land or in shallow water, *Polypterus* lift their heads by planting their pectoral fins in a contralateral pattern one after the other, and using large body

and tail oscillations, to push themselves forward over the planted fin (Standen et al., 2014). Moreover, *Polypterus* show flexibility and perform different walking strategies in response to different substrates. On smooth substrates, they walk as described above. However, on rough substrates, they opportunistically use the body to push off the substrate and irregularly use fins for stabilization (Standen et al., 2016). The robust and complex pectoral fin musculoskeletal structure may help *Polypterus* support their body when walking on land (Standen et al., 2016). In addition, *Polypterus* has been used in various studies where they have been held for extended periods on land. This change in environment resulted in a strengthening of the pectoral girdle bones which is similar to what is seen in the fossil record (Standen et al., 2014). Terrestrial acclimation also elicits a change from aerobic to glycolytic muscle fibers in the pectoral fin muscles (Du & Standen, 2017).

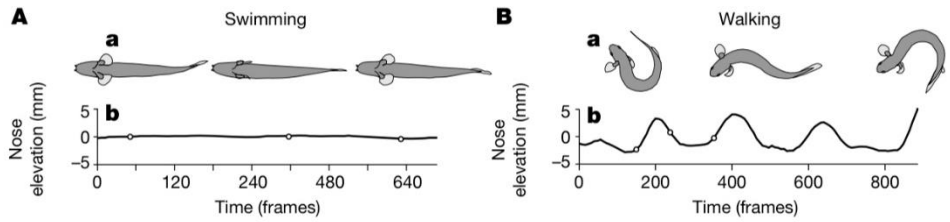

Figure 1.3: Aquatic and terrestrial locomotion of aquatic raised *Polypterus* (Standen et al., 2014). (A) shows a steady swimming kinematic pattern of Polypterus. (B) shows a walking kinematic pattern of *Polypterus*

Preliminary work on muscle activation patterns in fin musculature indicates double bursts in the adductor muscle during terrestrial walking (Foster et al., 2018). The appearance of double bursts on land could help stabilize the fin steps when contracting with an antagonistic muscle. Additionally, the pectoral adductor muscle shows greater muscle activation duration and amplitude during walking compared with swimming (Foster et al., 2018). However, there is no information on muscle activation patterns in the other three pectoral muscle groups. This study will quantify muscle activation patterns during walking and swimming for all four muscle groups in *P. senegalus* to gain an understanding of how muscle function changes in response to a novel terrestrial environment.

The forces that the fish experience in an aquatic environment are very different from those experienced in a terrestrial environment. In water, the movement of *Polypterus* is facilitated by buoyancy, and therefore, it does not require a huge amount of force production to maintain the movement compared to walking. On land, the fish bear more mechanical loading due to gravity. Unlike in water, the fish need to produce greater force for bearing the bodyweight when lifting the head off the ground. When the fin is planted on the ground, it is likely experiencing a ground reaction force, which requires a great contraction strength in the muscles when stabilizing the step. Therefore, more forceful contractions are needed in the pectoral fin muscle when walking on land compared to swimming in the water. Such heavy mechanical loading could lead to a selection of fast type fibers for a functional advantage in force generation when walking on land.

1.4 Fin muscle fiber type and muscle plasticity

Like other mammals, *Polypterus* have three muscle fiber types in the pectoral fin: red, pink, and white (Du & Standen, 2017). Red muscle fibers have abundant myoglobin for oxidative activity and low anaerobic activity, yielding high endurance and fatigue resistance (Herbison et al., 1982; Schiaffino & Reggiani, 2011). These fibers tend to contract for a longer duration and are referred to as slow-twitch muscles (Herbison et al., 1982). Whereas, white muscle fibers have a lower myoglobin content with less oxidative activity and higher lactic acid build-up, so they are easily fatigued (Herbison et al., 1982; Schiaffino & Reggiani, 2011). White muscle fibers tend to contract quickly and are referred to as fast-twitch muscles (Herbison et al., 1982). In comparison to red muscle, the white muscle contracts much faster and produces higher muscle force. Thus, it is mainly used in discrete burst swimming (Jayne & Lauder, 1993, 1994). Pink muscle is the intermediate muscle fiber type between red and white muscle. Fiber transition between white and red muscle fiber occurs when there is a change in exercise training (Pette, 1998), neuromuscular activity, and mechanical loading. Moreover, the conversion of white to red muscle fiber is in response to high endurance training (Wilson et al., 2012). Whereas, the conversion of red to white muscle fiber is in response to strength exercise and high-velocity isokinetic contraction, like ballistic movement (Wilson et al., 2012). Inherently, the increased usage of specific muscle fiber type(s) would eventually shift muscle fiber composition towards the most used muscle fiber type for effectively achieving the desired kinematics. Likewise, the switch to white muscle fibers in terrestrially reared *Polypterus* (Du & Standen, 2017) could be induced by the change in exercise and muscle demand from water to land.

1.5 Mechanical function of muscles: Force-length curve and force velocity curve

The force-length curve (FLC) of a muscle describes the relationship between muscle length and the amount of force it produces at that length. A sarcomere is the functional unit of striated muscle. It contains a specialized organization of actin and myosin filaments that actively pull on one another in a ratcheting motion. When muscle elongates or shortens, the filaments slide away from or toward the M line (the center of the sacromere) to generate contractile force (Mansfield & Neumann, 2019). The myosin filaments have different polarities on the head and tail. The sarcomere unit produces forces by transferring chemical energy (via ATP hydrolysis) to mechanical energy when the polar side of myosin binds to actin (Plowman & Smith, 2007). The stretched length of the muscle determines the overlap of myosin and actin filaments and impacts how much force can be produced during activation (**Figure 1.4**). Unfortunately, *Polypterus* pectoral fins are too small and thin for direct muscle length measurement of the four muscles of interest. If a single muscle is treated as muscle fiber, the relative amount of force that it tends to produce can be estimated. Force production capabilities based on muscle length varies between species due to differences in sarcomere length (Gordon et al., 1966). In an ideal world (**Figure 1.4),** the muscle yields maximum force within a resting muscle length as the filaments completely overlap. Within approximately 70%-130% of the resting muscle length, muscle tension starts decreasing when muscle shortens or elongates away from the range of optimal resting length.

When the muscle is beyond 70%-130% of the resting length, muscle tension starts decreasing rapidly and the muscle starts to be damaged. The force production drops to zero when it is maximally compressed or stretched (60%-170% of the resting length), and the muscle is further damaged and cannot develop tension (Gordon et al., 1966; Infantolino et al., 2010; Rassier et al., 1998). Resting muscle length can be measured when the animal is at rest without muscle activation. Operating length measures muscle length relative to resting length, which indicates where on the force-length curve a muscle is operating at a given moment in time. If the range of operating lengths exceeds the normal range, the muscle will risk being damaged. Therefore, operating length could allow estimation of the force output during muscle length changes.

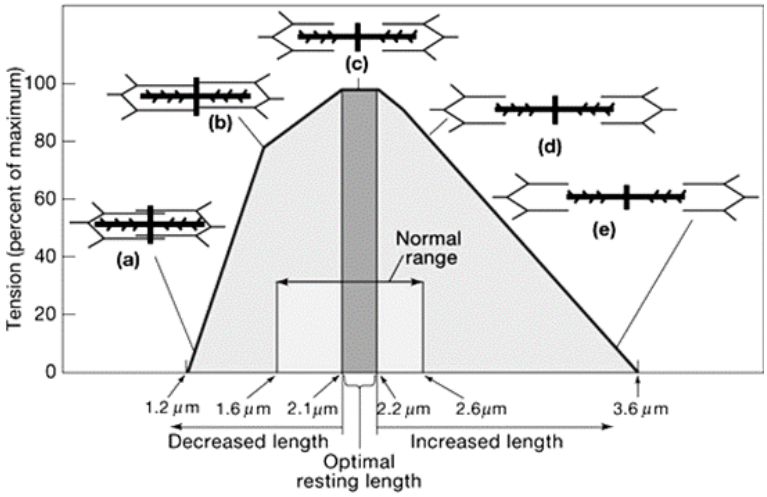

Figure 2.1: Force length curve of a sarcomere with schematic diagram of the sliding filament theory. (a)-(e) represent various levels of actin-myosin overlap. The graph demonstrates muscle tension changes from most compressed to most extended sarcomere. At point (a), tension is nearly zero when titin is extremely compressed. From (a) to (b), and (b) to (c) (ascending limb), tension increases with increasing length due to decreased myosin blockage. The flat line (including pint (c)) is the plateau region with maximum tension. At the descending limb ((d) to (e)), tension decreases when myosin filaments are stretching apart. Muscle force eventually falls to zero when the sarcomere is stretched such that there is no actin-myosin overlap (point (e)) (Picture borrowed from Power, 2014).

The force-velocity curve (FVC) describes another property of muscle function for quantifying muscle efficiency and fatigue (**Figure 1.5**). It demonstrates how the force output varies with contraction velocity (isotonic and isometric contraction). Isotonic contractions can be either eccentric or concentric. When the muscle elongates while active (eccentric contraction), force production increases with increasing velocity, and overall force generated by eccentric contraction is higher than isometric contraction. Whereas, when a muscle shortens while active (concentric contraction), force production decreases with increasing velocity, and overall force produced by concentric contraction is lower than isometric contraction (Fenwick et al., 2017). Essentially, it suggests that when muscle rapidly shortens, the muscle cannot produce a great amount of force. Since the pectoral fin locomotion of walking is very distinct from swimming in

Polypterus, we may better understand the mechanisms of fiber damage after short-term walking and fiber transition after terrestrial rearing by investigating how muscle properties change between the two behaviours.

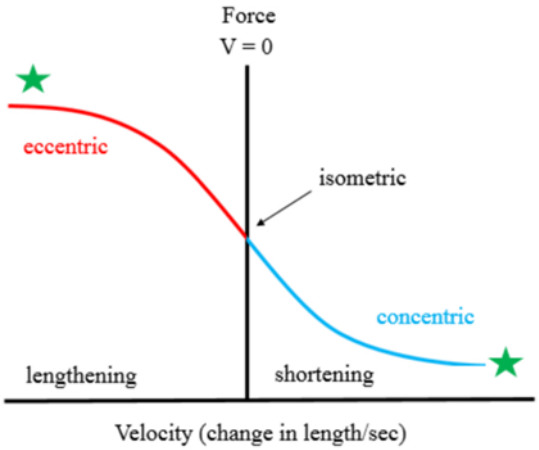

Figure 2.2: General force-velocity curve of a muscle. The graph shows that when increasing velocity, force increases in the eccentric contraction region (in red). When increasing velocity, force decreases in concentric contraction region (in blue). When x=0, it demonstrates isometric contraction where force remains unchanged with zero velocity. The green stars highlight the asymptotic regions where there is no force change with further velocity elevation (borrowed from Dhuper (2018)).

1.6 Mechanisms that lead to muscle damage

Muscle damage can occur via overstretching, during eccentric exercise, and after prolonged exercise. During an eccentric contraction, muscles are active during lengthening which stiffens the muscle and restricts movement. However, such contractions usually lead to muscle fatigue and damage as sarcomeres are overstretched when the muscle is forcibly lengthened (Morgan et al., 1999) Prolonged use of a muscle without a chance to recover also leads to fatigue and damage as muscle metabolites build-up (Appelt et al., 1992; Del Coso et al., 2012). Finally, overstretching muscle, while active or passive can lead to micro-tearing and damage as well (Garrett, 1996). Looking at the difference in muscle usage between swimming and instantaneous walking can help understand explain muscle damage in *Polypterus* after acute walking.

.

1.7 Potential drivers of muscle plasticity in *Polypterus* and hypothesis

Previous work has suggested that muscle fiber type changes from red to white in the pectoral fins of land reared *Polypterus* are due to changes in muscle activation pattern and effort (Trina Y. Du & Standen, 2017; Foster et al., 2018). The change in motion of the fin while walking suggests that the pectoral fin muscles in *Polypterus* might generate a greater amount of force or contract at a faster rate compared with swimming. In addition, a study on the muscle damage associated

with a single bout of walking in aquatically raised animals resulted in increased staining by Evan's Blue Dye (Dhuper, 2018). This dye enters damaged cellular membranes staining damaged cells blue. Interestingly, the most damage was found in the adductor muscle. These studies combined suggest that muscle function changes asymmetrically between fin muscles during walking. The simultaneous measurement of muscle activity of all four muscle groups conducted in this project can help better understand muscle functional changes and help explain possible mechanisms behind muscle damage and plasticity seen in the literature.

Using high-speed video and electromyography, this thesis will quantify how changes in kinematics and muscle activation contribute to muscle functional performance and provide mechanisms that explain both short-term and long-term changes in muscle physiology. I hypothesize that fin motion combined with muscle activation timing and intensity critically alter muscle physiological function. I predict that during walking muscle intensity, duration, and effort will increase and the adductor muscle will shift towards eccentric contraction.

Chapter 2: muscle activation of fin musculature in *P. senegalus* during swimming and walking.

2.0 Abstract

Previous studies have shown significant differences between walking and swimming in the locomotion patterns of the amphibious fish, *P. senegalus*. Particularly, pectoral fins increase their range of motion and change from moving in a synchronized motion to a contralateral motion when walking compared with swimming. *Polypterus* has a complex pectoral musculature consisting of four muscle groups: abductor, adductor, zono, and coraco, which appear intermediate between fish and tetrapods. How the pectoral muscles in *Polypterus* change their function to accommodate the change in behaviour between walking and swimming is unknown. Fin anatomical studies of fish exposed to walking environments show short-term damage to specific fin muscle groups and longer-term musculoskeletal plasticity. Differences in the detailed fin kinematics and full muscle activation patterns between walking and swimming *Polypterus* may help explain the physiological and anatomical changes that are seen in fish raised on land. The goal of this work is to understand the mechanisms driving phenotypic plasticity and changes in general muscle function seen in fins used for terrestrial locomotion. This study uses high-speed videography and electromyography to compare muscle function between walking and swimming behaviours in *P. senegalus.* Muscle activation patterns in all four groups of fin muscles show the largest changes in function occur within the adductor muscle, where increases in the timing and duration of muscle activation during walking may explain damage and muscle fiber changes seen in previous studies. This work begins to clarify how mechanical advantage changes between drastically different locomotion impacting muscle performance and improving our understanding of the mechanisms driving phenotypic plasticity in an amphibious fish.

2.1 Introduction

Before the evolution of tetrapods, early fishes may have used their fins to explore terrestrial environments. *P. senegalus* is the basal-most extant actinopterygian which is the sister group to sarcopterygian fishes including tetrapods (Betancur-R et al., 2017; Suzuki et al., 2010). Using the extant *P. senegalus* as a model, I aim to understand how fin function changes between aquatic and terrestrial environments. The pectoral fins of *Polypterus* are lobe-like and have a complicated musculature (Wilhelm et al., 2015), allowing for terrestrial locomotion (Du & Standen, 2017; Standen et al., 2014, 2016). After being placed on land for an extended period, these fish demonstrate behavioural plasticity, becoming more effective walkers and developmental plasticity generating supportive bone structures for weight-bearing (Du & Standen, 2020; Standen et al., 2014). The bones of the pectoral girdle change shape with a tighter connection between cleithrum and clavicle (**Figure 1.1 A**), resembling the change in the stem tetrapods (Standen et al., 2014). Fin bones also change with exposure to terrestrial environments. The propterygium and metapterygium (see the anatomical position in **Figure 2.1 E**) become longer and wider, and the metapterygium becomes more ossified in response to the terrestrial mechanical loading (Du & Standen, 2020). These previous observations suggest that the pectoral fin of *Polypterus* is a good model for understanding how ancestral fish might have used its fins to

walk on land. To overcome the challenges due to novel environmental constraints and walk more effectively, the ancestor must have the ability to modulate its muscle structure and function, especially in the fin. Phenotypic changes were found in the pectoral fin muscle between water-raised and land-raised fish. The pectoral fin responds to the environmental change by changing its muscle fiber types following acclimation (Du & Standen, 2017; Dhuper, 2018), and muscle activation pattern during acute walking (Foster et al., 2018), suggesting a functional change in the fins. This study focuses on the pectoral fin muscle of *Polypterus,* seeking to understand what drives the phenotypic changes in pectoral fin muscle induced by the novel terrestrial environment.

The pectoral fin musculature of *Polypterus* consists of six muscles (**Figure 1.2**). Because of the extremely small size and similar positioning of these muscles they have been categorized into four groups: zono, abductor (abd. sup. and abd. pro combined), coraco (coraco I and II combined), adductor (see **Figure 2.1**). As in **Figure 2.1 A**, zono originates from the scapulocoracoid and inserts onto the distal propterygium that articulates with the small distal radials connecting to the fin rays. Based on this anatomical position, zono is responsible for elevating the fin. Both abductor (**Figure 2.1 B**) and adductor (**Figure 2.1 D**) originate on the scapulocoracoid and insert on either side of the very thin fin at the base of the fin rays. Although they have similar insertion, their origins are slightly different. Abductor originates from the lateral and dorsal part of the scapulocoracoid while abductor originates from the medial part of the scapulocoracoid, making the two muscles anatomically opposed to each other. When the muscles contract, the abductor muscle acts for abduction and pronation while the adductor acts for adduction. As in **Figure 2.1 C**, the coraco originates from the scapulocoracoid and inserts onto the metapterygium whose distal side articulates with the small distal radials connecting to the fin rays. Contracting the coraco likely results in fin depression. These muscles all wrap around the convex glenoid joint on the pectoral girdle at the fin base (**Figure 2.1 B**), which has similar functionality to the tetrapod shoulder joint. This skeletal structure provides better control for fin rotation, potentially allowing the fish to perform complex locomotion in response to various environments. During steady rectilinear swimming at slower speeds, *Polypterus* move the pectoral fin back and forth synchronously to generate thrust while keeping their body straight (Standen et al., 2016). During walking, *Polypterus* move the pectoral fins contralaterally which helps lift the head and forebody off the ground (Standen et al., 2016). After being raised in a terrestrial environment, the fish change morphologically, particularly, in the head and pectoral fin bones. Their pectoral girdle bones become more supportive and the pectoral fin bones become longer and more ossified compared to aquatic fish. As a result, the terrestrially reared *Polypterus* walk more effectively (Standen et al., 2014). These changes in the bones could be induced by the dramatic change in forces experienced by the fish when switching from aquatic to terrestrial environments.

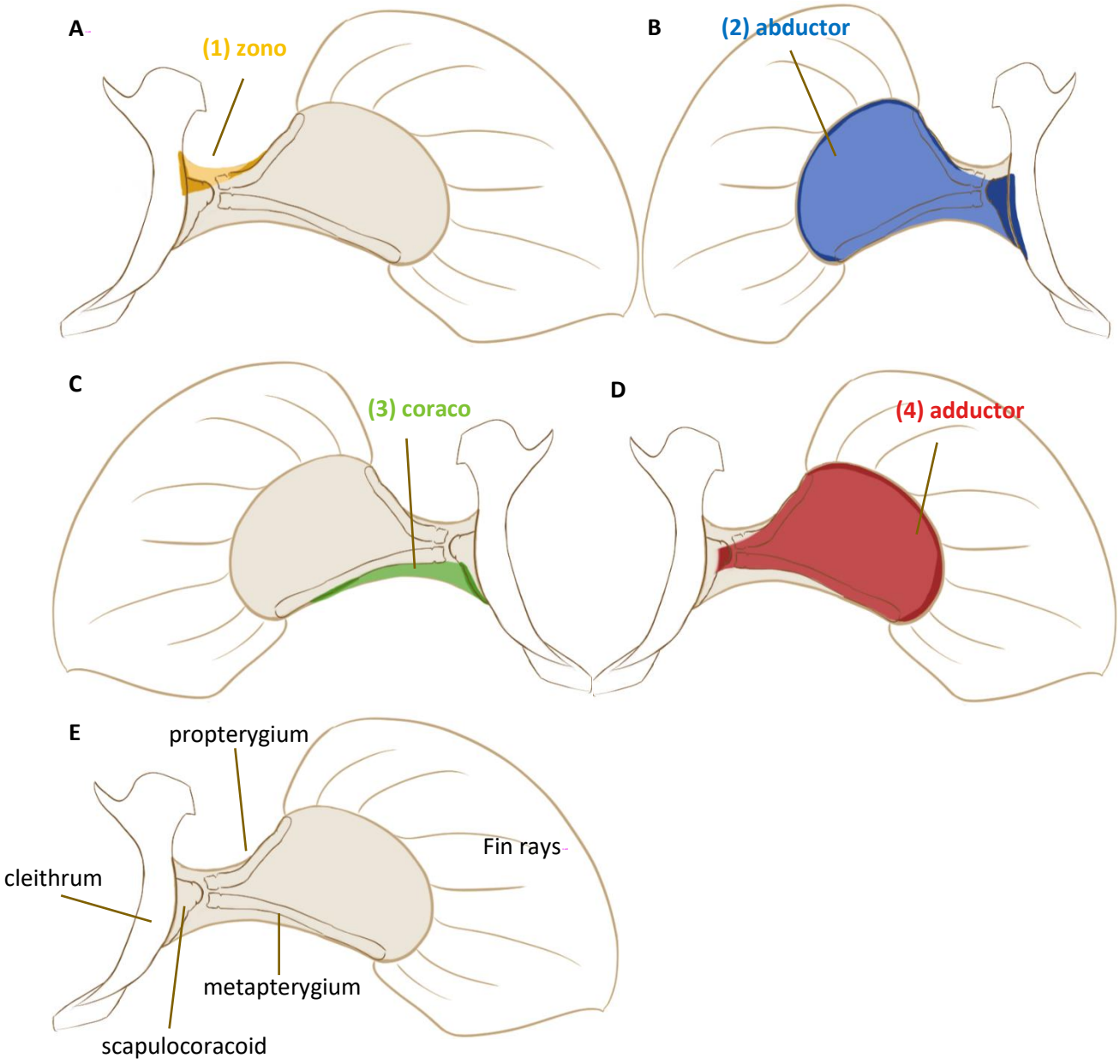

Figure 3.1: Illustrated anatomy of the left pectoral fin in *P. senegalus*. (A) the yellow muscle illustrates the position of zono (electrode (1)). **(B)** the blue muscle illustrates the position of abductor (electrode (2)). **(C)** the green muscle illustrates the position of coraco (electrode (3)). **(D)** the red muscle illustrates the position of adductor (electrode (4)). All the fin muscle colours correspond to the colour labeling of the EMG traces (**Figure 2.2**). **(E)** illustrates the pectoral fin musculoskeletal structure without highlighting the muscles. **(A), (D), (E)** are presented from the posterior view (looking from medial/inside of the fin), and **(B), (C)** are presented from the anterior view (looking from the lateral/outside of the fin). The anatomy is illustrated based on the study by Wilhelm et al. (2015).

Following walking, muscle damage was detected in the pectoral fin of the *Polypterus*. In undamaged cells, Evans Blue Dye that is injected into the muscle stays in the extracellular matrix. In contrast, cells with damaged membranes allow the dye to enter the cells, highlighting muscle regions with damaged cells. After a single bout of walking, the damage was seen across all muscles, except for the coraco muscle. Interestingly, the most severe damage was visible in the adductor muscle. Within the walked fish, there was an increase in the abductor and the zono muscle damage from proximal to distal, whereas the adductor had the most damage proximally (Dhuper, 2018). Both the magnitude and distribution of the adductor muscle damage compared with other fin muscles suggests it has the largest functional change in the transition from swimming to walking.

The pectoral fins not only show muscle cells are damaged during walking, but also show morphological changes after walking for a long time. After housing fish on land for two months, *Polypterus* shows a muscle fiber type transition in the pectoral fin. All four fin muscles increased their white muscle fiber content and showed compartmentalization between red and white muscles(Du & Standen, 2017). This fiber transition suggests a possible change in neuromuscular activity. The compartmentalization is more distinct at the ventral edge of the fin which is the side that tends to land on the ground. In addition, the abductor has a smaller red muscle fiber portion than the other muscles. Looking from distal to proximal, white muscle fiber content increased in the abductor muscle in land-raised fish, but decreased in aquatic fish, suggesting that there is a change in role from swimming to walking (Du & Standen, 2017). White muscle fiber is known for fast contraction and strong mechanical power. Whereases, red muscle fiber is known for slow contraction but high endurance, and resistance to fatigue (Schiaffino & Reggiani, 2011). A switch in muscle fiber type could suggest a change in muscle function.

To understand muscle functional changes more fully, knowing how muscle activation patterns change during different locomotor motions is important. There is only one study to date that looks at adductor muscle activation patterns alone, showing that the timing and magnitude of muscle activation changes between swimming and walking (Foster et al., 2018). Nothing is yet known about the combined function of the four muscle groups that control fin motion. Given the changes in morphology and locomotor behaviour in this system, understanding the fin muscle function of *Polypterus* is of importance for understanding how morphological and behavioral plasticity can facilitate movement in novel environments. In this study, I intend to look at the differences in the detailed fin kinematics and full muscle activation patterns between walking and swimming in *P. senegalus*. This will give us insight into how the fin muscles work within two different locomotor modes. Through this study, I am aiming to gain a better understanding of what causes muscle damage and fiber type transitions in *Polypterus*. Therefore, I hypothesize that: (1) a change in muscle activation patterns drives muscle damage; (2) a change in muscle activation patterns favours muscle fiber transition.

2.2 Materials and Methods

2.2.1 Subjects

Three adult *P. senegalus* Cuvier 1829 [mass = 15.13 ± 0.77 g; total length = 14.13 ± 0.41 cm)] were obtained from the pet trade (Mirdo Importations Canada, Montreal, QC, Canada), and acclimated in the University of Ottawa Aquatics Facility. The fish were kept in an aquatic environment in a 12L:12D light cycle with a high protein diet. Prior to each experimental trial, all the fish were acclimated for at least two weeks and were not fed within 24 hours before surgery. *Polypterus* observation, care, and experimentation were conducted in accordance with the University of Ottawa Animal Care and Use Protocol no. BL3625.

2.2.2 Experimental procedures

Fish were anesthetized in 200 mg/L MS-222 (tricaine methanesulfonate) solution before electromyography (EMG) electrode implantation surgery. The fish were kept in the solution until they were unresponsive to tail pinching and their breathing slowed down. Each fish was placed in the resting zone of the filming tank filled with freshwater for recovery following the surgery. After the fish regained consciousness and started moving, it was moved to the filming zone and allowed to swim freely. Then, the fish was given a 1–2-hour break for recovery from the previous exercise before it was released to walk voluntarily. During swimming trials, the filming tank was filled with fresh water to a depth of 5 cm. During walking trials, the tank was drained fully, with the exception of a water-filled trough at one end, in which the fish could rest between walking bouts. Steady and continuous bouts of swimming and walking were recorded for each fish. Trials, where the fish took at least 3 consecutive strokes, were used and approximately 10 strokes of each behavior were analyzed for each fish. Fish were filmed at 500fps (frame per second) from the bottom and the side using two high-speed Photron Fastcam Mini UX100 cameras (Photron USA, San Diego, CA, USA). Camera views were calibrated using custom DLTdv8a software and videos were digitized to calculate 3D kinematics of walking and swimming behaviour (Hedrick, 2008).

2.2.3 EMG electrode placement

Electrodes were made from bi-filament coated stainless steel electrode wire (diameter: 0.051mm; California Fine Wire Company, Grover Beach, CA, USA). The insulation of the electrode tips (~0.5 mm) was removed, and the filaments were separated. Following separation, they were bent to create a hook-like structure, which helps to hold the electrode in place during animal locomotion. Four electrodes were percutaneously implanted into four muscle groups: zono, abductor, coraco, and adductor, as shown in **Figure 2.2** and **Figure 2.3**, using sharp 30-gauge needles. To minimize the impact of electrode implantation on normal locomotory behavior, only four additional body electrodes were placed in each fish. Three electrodes were placed on the left side and one electrode was placed on the right side of the body just under the skin surface (as demonstrated in **Figure 2.2**), in the red muscle slightly above and along the lateral line (25-gauge needle). After filming swimming and walking behaviours, the animal was euthanized with an anesthetic overdose (250 mg/600 ml MS-222). The fish was transferred to a dissection tray and carefully

dissected under a dissection microscope to confirm electrode placement. As stated above, the electrode implantation was confirmed, and the electrodes were placed at standardized locations to ensure the electrode locations are equivalent across fish of different body sizes.

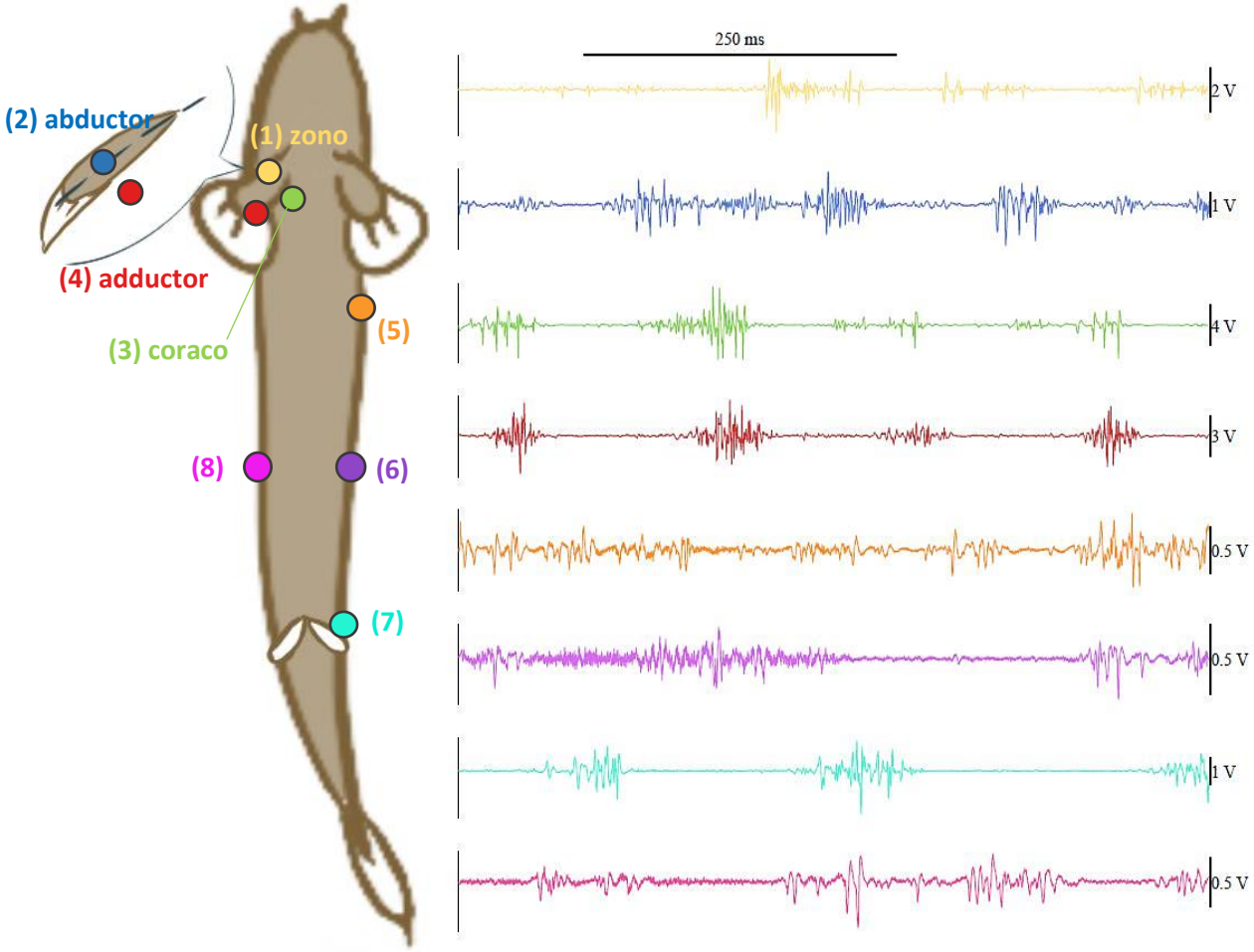

Figure 2.2: Ventral view of the pectoral fin and the body with corresponding muscle activation signal. A swimming fish is illustrated from a bottom view (the ventral side of the fish) with a representative EMG trace. The electrode placements are: (1) zonopropterygialis (zono), (2) abductor, (3) coracometapterygialis (coraco), (4) adductor, (5) left side of body, posterior edge of pectoral fin, (6) left side of body (½ of the way between (5) and (7)), (7) left side of body at the anterior edge of the anal fin, and (8) right side of the body which is the opposite side of electrode (6). All the body electrodes were implanted 1mm above the lateral line to maximize placement in red muscle. All the EMG traces are colour coded within the image.

2.2.4 Digitization

The three-dimensional kinematics of the fish were digitized using DLTdv8a (Hedrick, 2008) for MATLAB (version R2020a, The MathWorks, Natick, MA, USA). Digitized points are indicated in **Figure 2.3**. The tip of the nose (point 1), the tip of the tail (point 2), the tip of the right fin rays

(point 3), and the base of the fin (representing the lateral side of scapulocoracoid; point 4) are used to define the shape of the fish and indicate the position of the pectoral fin relative to the body. Four additional points on the right pectoral fin were used to locate the insertion points of the four major fin muscles. Point 5 represents the middle of the insertion of both abductor and adductor muscles. Point 6 indicates the zono insertion, placed at the dorsal edge of the fin lobe that meets the fin rays. Point 7 represents the coraco insertion which sits at the easily recognizable landmark where the ventral edge of the fin lobe meets the fin rays (**Figure 2.1**).

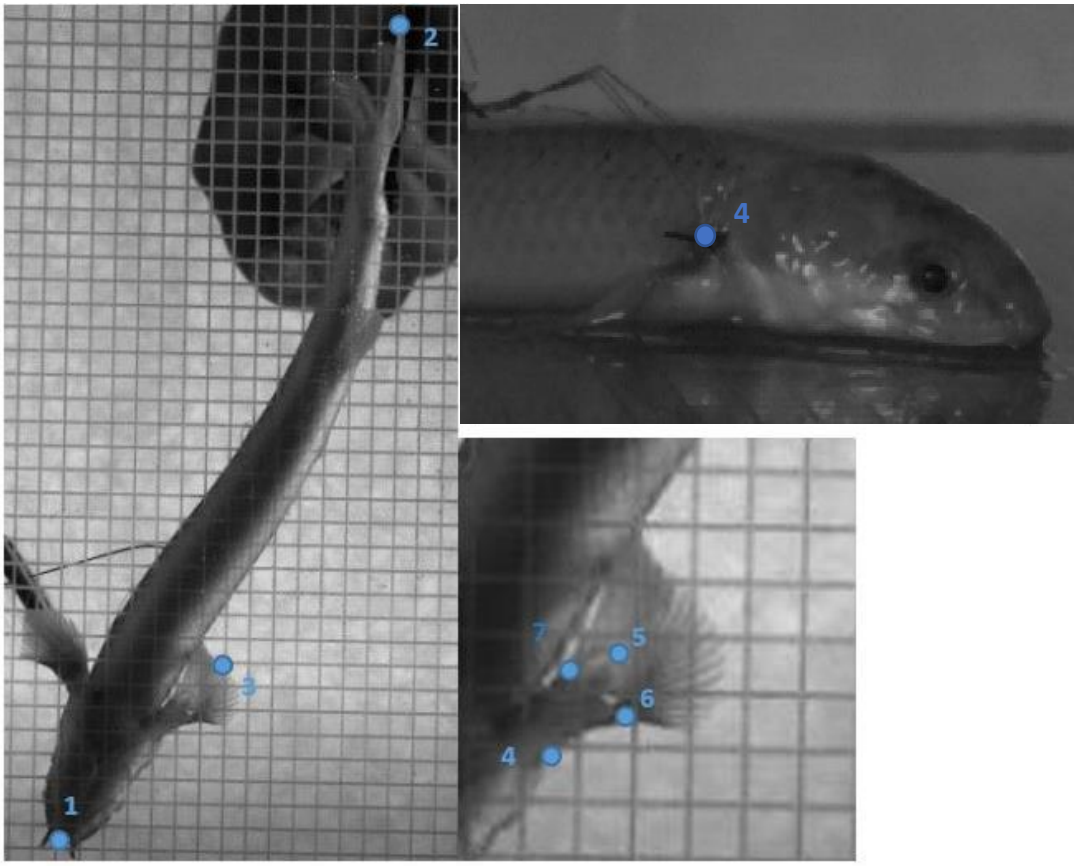

Figure 3.3: Digitization points on the body and the right pectoral fin. There are seven digitization points on the fish: 1. nose (the middle between the two nostrils), 2. tip of the tail, 3. pectoral fin tip (the tip of the fin ray), 4. pectoral fin base (digitized on the suture knotted on the dorsal/top side of the fin base next to the gill), 5. adductor, indicated by the middle of the distal edge of the right pectoral fin lobe (represents both adductor and abductor), 6. zono indicated by the dorsal edge of the end of the fin ray), 7. coraco, which is indicated by the ventral edge of the end of the fin ray. All the fin digitization points are on the right pectoral fin which is the same side where the electrodes were placed.

2.2.5 Electromyography variables

The muscle activity and kinematics were synchronized by an external trigger. The EMG signals were collected at 10 kHz using an AD Instruments PowerLab 16/35 data acquisition system (ADInstruments, Colorado Springs, CO, USA). The signals were amplified by 5,000 times and filtered with a 60 Hz notch filter using GRASS P511 AC amplifiers (Natus Neurology, Warwick, RI, USA). Background noise and unwanted signals were filtered out with a bandpass filter (40-4,000 Hz) in MATLAB (version R2020a, The MathWorks, Natick, MA, USA). Electronic devices during the setup (amplifier, lights, and camera) were grounded to further reduce electrical noise. Calculations of the magnitude variables were computed after the background signal noise was subtracted from the raw EMG data and the signals were rectified.

Onset and offset timings, activation duration, EMG duty factor, maximum burst amplitude, RIA (rectified integrated area), THRIA (time to reach half RIA), and the differences between swimming and walking for activation duration, maximum amplitude, RIA, and THRIA of each of the channels were obtained and calculated using custom MATLAB code, following the same method as Foster et al. (2018). Onsets and offsets were identified using the threshold of two times the standard deviation of the baseline signal of each of the channels as a guide (Roberts & Gabaldón, 2008). The baseline signal is an inactive portion of the EMG trace in each channel. Muscle activation onsets were selected manually when the EMG signal rose above 2x baseline at the start of a profiled burst. The offsets were selected when the signal fell below 2x baseline in a profiled burst. Onset and offset timings are expressed in polar coordinates (radians) relative to the corresponding fin stroke, as in **Figure 2.4 C & D**. Activation duration is measured as the absolute time in seconds between onset and offset timings. EMG duty factor is the percentage of the stroke cycle when the muscle is active (activation duration divided by fin cycle duration).

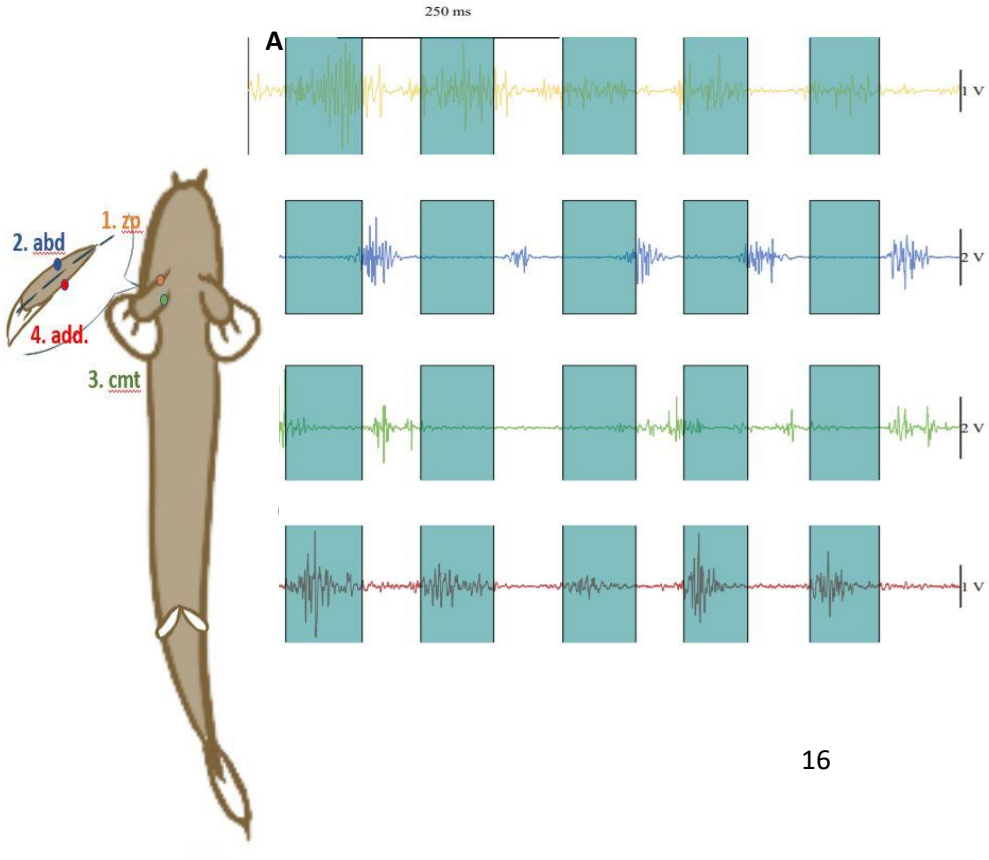

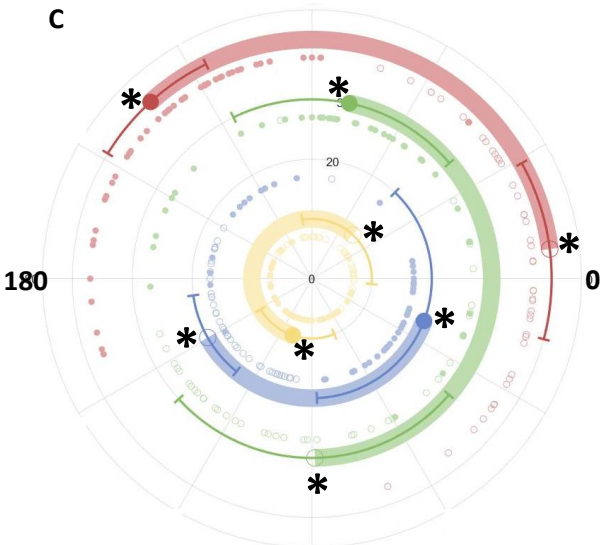

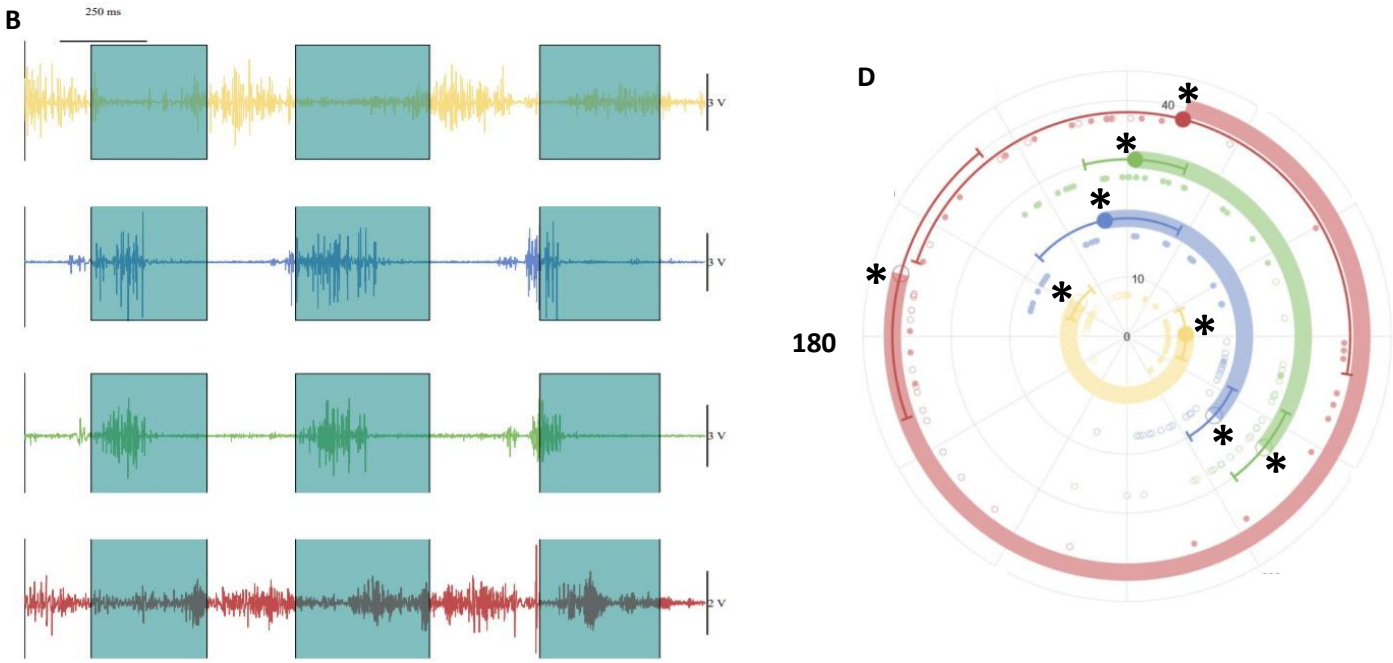

Figure 3.4: Timing of fin muscle activation in *P. senegalus* during walking and swimming. Muscles represented are 1. zono (yellow), 2. abductor (blue), 3. coraco (green), and 4. adductor (red). Example electromyography recordings of the right fin muscles are shown during one representative swimming (A), and walking (B) trial (shaded area = power stroke/adduction (swimming) or stance (walking); unshaded area=recovery stroke/abduction (swimming) or swing (walking)). The timing of fin muscle burst onsets and offsets relative to fin stroke cycle for swimming (C) and walking (D) behaviours are shown. The paler coloured thick lines indicate time during which muscle is active, from angular mean of onset (unfilled circle) to angular mean of offset (filled circles). Narrow lines indicate angular variance of onset and offset times. The small paler shaded points are individual data of onset and offset times. Beginning of the fin stroke (when adduction/stance phase starts) is 0 degrees and the middle of the fin stroke (when abduction/swing phase starts) is 180 degrees. The stroke progresses in a counterclockwise direction. Values are angular means ± angular variance. Asterisks indicates the statistically significant directionality of each temporal variable, and p-values are reported in **Table 3.4**.

An EMG signal represents the sum of electric potential produced by the muscle fibers around the electrode. Slight differences in the construction and placement of EMG electrodes mean that the raw signal from each electrode cannot be compared directly. To facilitate comparisons across muscle channels and fish, maximum burst amplitude and burst RIA are normalized by expressing them as a percentage of the absolute maximum measure for each channel observed in a reference trial with steady motion for each individual. The maximum amplitude of each burst within a stroke cycle was calculated as a mean of the top 5% of values for each muscle burst and reported as a percent of the maximum amplitude. Rectified integrated area (RIA) is the area under the rectified (i.e. the absolute value of the signal) curve of the EMG signal for each muscle burst. Within each burst, all the signals are converted to the absolute value as when being

rectified. The area underneath the rectified signals is RIA. RIA is expressed as a percentage of the theoretical maximum RIA (maximum amplitude times duration for a given burst) to estimate muscle effort in this study. THRIA is the time that the muscle takes to reach half of the RIA achieved in a burst and represents the shape of the muscle burst (Foster and Higham, 2014). The THRIA is expressed as a percentage of activation duration.

Differences in EMG variable magnitudes between swimming and walking behaviours were calculated for each fish by subtracting the estimated marginal mean (emmean) of walking from swimming. A negative value indicated an increase in walking while a positive value indicated a decrease in walking. The emmean and standard error of the mean (s.e.m.) of all the magnitude variables, and the 95% confidence intervals of all EMG difference variables were calculated based on the corresponding fitted linear mixed-effects (LME) models in R (reported in **Table 3.2** & **2.3** and **Appendix Table 1** & **2**).

2.2.6 Kinematic variables

The stroke cycles for swimming and walking were defined by the motion of the pectoral fins. In swimming, the start and end of the fin stroke cycle were determined by maximum fin abduction, and the middle of the cycle was determined by maximum fin adduction. In walking, the start of the stance phase (when the fin was first loaded on the ground; close to maximum abduction) represents the start of the cycle, the end of stance or start of swing phase represents the mid-cycle (approximately at maximum adduction). The speed of fish movement was calculated based on the movement of the center of mass estimated by the fin base point. Swing distance was calculated for the nose, head, tail, and tip of the fin based on the body point movement in a real-world space. It was the distance that each point traveled from the maximum amplitude on the right to the maximum amplitude on the left along the swing path (**Figure 2.5**). As described previously (Standen et al., 2014, 2016), *Polypterus* moved their head up and down during walking on land, whereas there was no vertical rhythmic movement of the fish head during swimming. Nose elevation was measured as the movement of the nose point along the z-axis over time. To understand how the fin muscle activation can be affected by the head movement, when the fish head was elevated and dropped to the ground was evaluated. As observed previously (Standen et al., 2014) and in this study, the nose elevation always had a double-peak during one fin stroke cycle. One nose elevation peak occurred during the stance phase, and another nose elevation peak occurred during the swing phase (of the right fin). When the right fin was placed on the ground, the left fin was in swing. So, the nose elevation peak during the stance phase must be driven by the right fin. Conversely, the head elevation during the swing phase must be driven by the left fin. The right fin, which was the fin implanted with electrodes, was used to measure the fin muscle activity and the detailed kinematics to understand the functional change between behaviours. To focus on the motor performance and muscle activity in the pectoral fin, we used the nose elevation peak during the stance phase only. The time at maximum nose elevation was when the nose reached a peak elevation during the fin stance phase. The time at minimum nose elevation followed directly after the time at maximum nose elevation when the fish head fell

directly back to the ground, which minimized noise in the elevation data that occurred as the nose bounced or slid across the substrate.

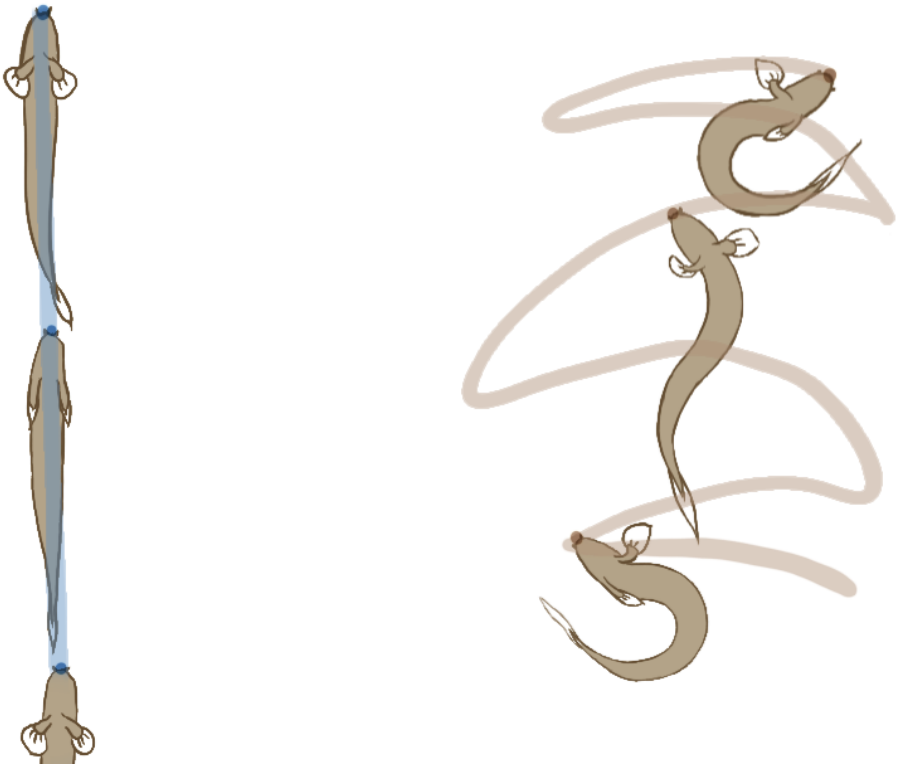

Figure 3.5: Illustration of the fish body swing path for swing distance calculation. Example of the movement path of the nose point is illustrated in a swimming fish (at the left) and a walking fish (at the right). The nose of the fish was steady during swimming and therefore, it yielded minimal swing distance, which was neglectable (see table in **Appendix Table 1**).

To evaluate fin motion in relation to the fish, all points were translated and rotated such that the line from fin base to nose represents the x-axis. The fin adduction angle was defined as the angle measured in degrees between the nose, fin base, and the abductor/adductor point on the x-y plane of the fish (**Figure 2.6 A**). Thus, the maximum adduction angle indicates full adduction while the minimum adduction angle indicates full abduction. The fin adduction angle range was calculated as the difference between the maximum and minimum adduction angle. The adduction angle range, maximum, and minimum adduction as well as the timing at full adduction and full abduction were collected for each fin stroke cycle. Fin elevation evaluates how much the fin was elevated or depressed by measuring the movement of the abductor/adductor point along the z-axis in relation to the fish fin base (**Figure 2.6 B**). To evaluate the vertical range of fin motion, the fin elevation range was calculated as the difference between the maximum and minimum values of fin elevation. The timings of the maximum, and minimum elevation (**Appendix Figure 5**) were expressed in polar coordinates relative to the pectoral fin stroke cycle (**Figure 2.8**).

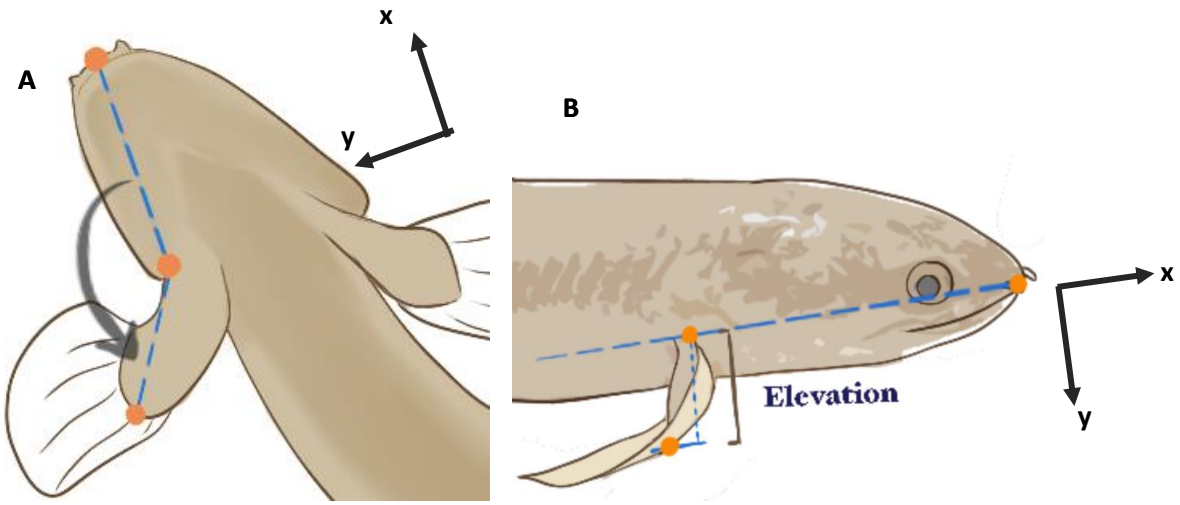

Figure 3.6: Schematic illustration of fin adduction angle (A) and fin elevation (B). Orange dots indicate the digitization points used for calculating the kinematic variables. (A) illustrates the fin adduction angle from a bottom view. (B) demonstrates the fin elevation from a side view.

The angular velocity of adduction and abduction were measured in the x-y plane as the mean of the highest 5% of values for the entire trial (**Figure 2.9 A**). These 5% maximum angular velocities were used to compare the extreme adduction and abduction speed between aquatic and terrestrial locomotion. Additionally, 'routine' fin speed was calculated as the mean value of the top 20% of angular velocities for adduction and abduction per trial. In other words, the 5% maximum velocity measures the fastest speed a fish could potentially reach, while the 20% maximum velocity measures the regular average fastest speed in each fin beat cycle. The different signs of the values represent different directions of fin movement. A negative value indicates fin abduction, while a positive value indicates fin adduction.

2.2.7 Statistical analyses

Linear mixed-effect (LME) models were conducted to evaluate the difference of each magnitude variable between behaviours. R studio (version 9.0, RStudio: Integrated Development for R. RStudio, PBC, Boston, MA) was used to perform the statistical analyses. All the magnitude variables are analyzed using linear mixed-effects models coded in a custom R script, and the results were reported as ANOVA-like tables for simplicity.

Random effects were modeled as trial nested in the corresponding fish to account for non-independence between behaviours taken from the same individual. Behaviour was a fixed effect for kinematic magnitude variables, and behaviour and muscle were fixed effects for EMG magnitude variables. Shapiro-Wilk test and Levene's test were used to test the normality and variance equality of the residuals before running pairwise comparisons on the data. Log transformation is applied to the data to transform any skewed data to approximately conform to normality. Any log-transformed emmean ± s.e.m. is inverse transformed for data presentation in the plots. Multiple comparisons were computed on the EMG magnitude variables to look at the difference between behaviours across muscles. Thus, p-values were adjusted by Bonferroni

correction to protect from type I error. The upper and lower 95% confidence intervals of the EMG magnitude differences between swimming and walking were compared across muscles. This comparison allows us to evaluate whether one muscle has a significantly different change from swimming to walking than another muscle.

Temporal variables were analyzed using circular statistics (Zar, 1999), following the same method as Standen *et al.* (2016) utilizing custom MATLAB code. The Kuiper test and Rayleigh test were utilized to detect the existence of von Mises distribution and directionality of the temporal data (Zar, 1999). When the data disobeyed von Mises distribution and had multi-modal distribution, the Hermans-Rasson test was applied as an alternative test to the Rayleigh test (Landler et al., 2019). Due to the sample size in this study, the two tests are applied to the temporal data pooled by behaviour. The distribution and directionality of the data on the fish and trial level were confirmed before running the Watson-Williams multi-sample tests. The Watson-Williams tests were used to compare the difference in angular mean between behaviours. Alternatively, non-parametric Watson-Wheeler tests were applied to the data that failed to meet the assumptions of the Watson-Williams test (Batschelet, 1981; Jerrold H. Zar, 1999).

2.3 Results

2.3.1 Fin muscle activation timings and fin kinematic performances in swimming and walking

In this study, the activations of all muscles (for both fin and body) are characterized as a distinguished single strong burst within a fin stroke cycle (**Figure 2.4 A & B**), except for the adductor during walking. The burst of activation in the adductor during walking was often an extended burst of variable shape with low signal intensity (**Figure 2.4 B**). Overall, the fin muscle activation pattern changes dramatically between swimming and walking behaviour (**Figure 2.4** and **Table 3.4**). During swimming (**Figure 2.8 A**), coraco and adductor activated during adduction/power stroke, and zono and abductor activated during abduction/recovery stroke, appearing to work as pairs. As in **Figure 2.4 A & C**, each of the muscles turn on one after another throughout the entire stroke. During walking (**Figure 2.8 B**), the activation timing of muscles changed to a different mode, especially the adductor. The adductor stayed active throughout the majority of the fin stroke cycle (**Figure 2.4 B&D**). Zono turned on at the end of the stance phase and remained active throughout the entire swing phase. Adductor turned on right after the zono muscle initiates activation and remained active throughout the entire swing phase and the first half of the stance phase. Note that although adductor onset was consistent (mean=2.3096±0.2809; **Table 3.4 & Figure 2.4 D**), adductor offset was relatively variable (mean=1.3176±1.4881; **Table 3.4 & Figure 2.4 D**). Coraco and abductor turned on almost simultaneously before the stance phase began to initiate the stance phase of the cycle along with the activation of adductor (**Figure 2.4 D**). As shown in **Figure 2.8**, nose elevation reached a maximum early in the stance phase and reached a minimum late in the stance phase.

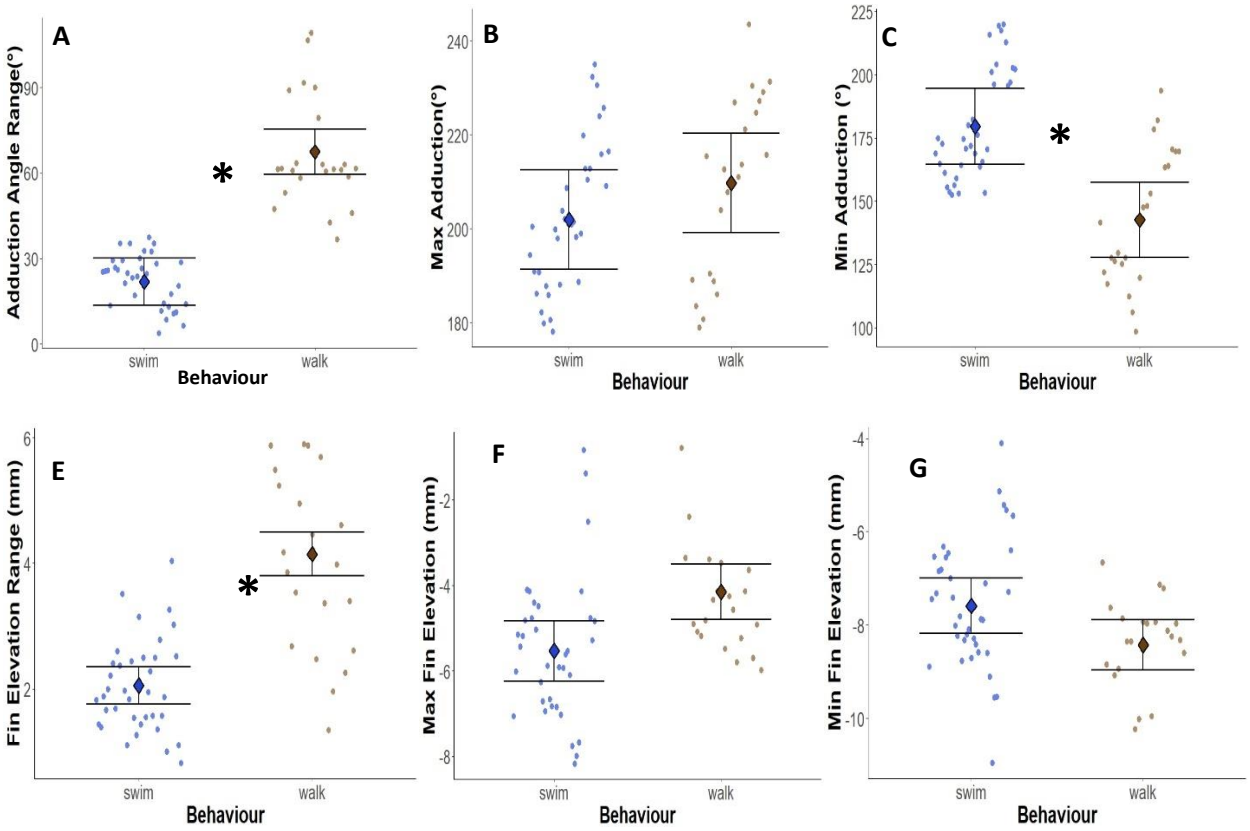

Figure 3.7: Differences in magnitudes of pectoral fin kinematic variables between swimming and walking. Blue and brown indicate swimming and walking, respectively. The small points are individual values of all the data. (A) the fin adduction angle range is expressed in degrees, calculated as the difference between maximum and minimum fin angles. (B) the maximum adduction was measured in degrees. Greater magnitudes indicate increased fin adduction. (C) the minimum adduction was measured in degrees. Smaller magnitudes indicate decreased fin adduction. (D) the fin elevation range is expressed in mm, calculated as the difference between maximum and minimum elevations. (F) the maximum elevation was measured in mm. Greater and smaller value indicate increased and decreased fin elevation. (G) the minimum elevation was measured in mm. Greater and smaller value indicate decreased and increased fin depression. All values are presented as emmean ± s.e.m. Asterisks indicate significant differences between swimming and walking behaviours (the p-values are reported in **Table 3.3**).

On average, the swimming and walking speeds of the fish were not significantly different (**Appendix Table 1**). The adduction angle range was significantly greater in walking than in swimming (**Figure 2.7 A**), which was mainly contributed by the significantly smaller minimum adduction (**Figure 2.7 C**). During walking, minimum adduction occurred while the adductor was active (**Figure 2.8 B**). The maximum fin elevation increased, and the minimum fin elevation decreased during walking, as shown in **Figure 2.7 F & G**. Although those changes were not significant, the two factors together contributed to a significant increase in the range of fin

elevation (**Figure 2.7 E**; **Table 3.3**). Interestingly, during walking, the minimum elevation timing was variable (P=0.86, **Table 3.4**) while the maximum elevation timing was consistent relative to the pectoral fin stroke cycles (P=0.034, **Table 3.4**). The pectoral fin tended to reach the maximum elevation near the end of zono activation during swimming (**Figure 2.8 A; Table 3.4**), but around the middle of zono activation during walking (**Figure 2.8 B; Table 3.4**). As in **Figure 2.9**, both the top 5% and 20% maximum fin adduction velocity were greater during walking. The 20% maximum fin adduction velocity of walking nearly doubled relative to swimming (**Table 3.3**). Generally, there was no significant difference in the timing of maximum and minimum adduction and elevation relative to fin stroke between behaviours (**Table 3.4**). During walking, maximum nose elevation occurred along with the activation of the abductor, coraco, and adductor, while the minimum nose elevation occurred at the void 'inactivation' zone (**Figure 2.8 B**).

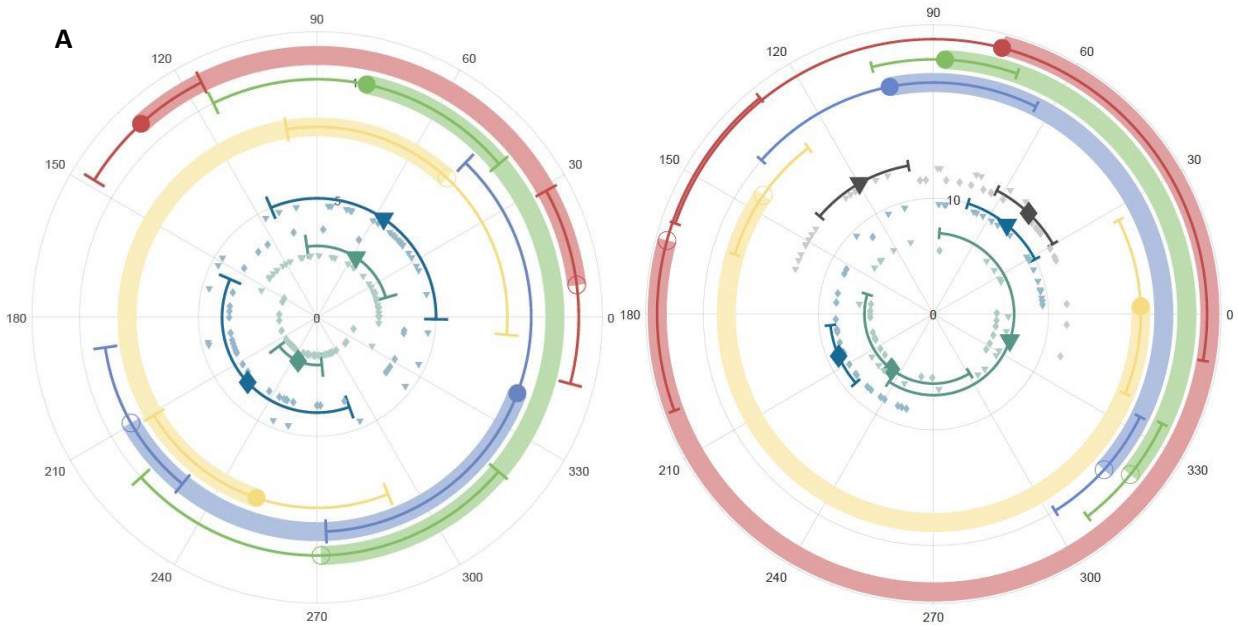

Figure 3.8: Kinematic temporal variables in *P. senegalus* during swimming (A) and walking (B). The small paler shaded points are individual values of the entire dataset. The timing of maximum and minimum fin adduction and elevation during swimming (A) and walking (B) are compared with fin muscle activation in relation to fin strokes. Beginning of the fin stroke (start of power stroke/stance phase) is 0 degrees and the middle of the fin stroke (start of recovery stroke/swing phase) is 180 degrees. The muscle activations are presented as thick lines in the same manner as **Figure 2.4** (zono=yellow, abductor=blue, coraco=green, and adductor=red). Black, dark green, and navy represent nose elevation, fin elevation, and fin adduction. Diamonds and inverted triangles indicate the maximum and minimum of the variables. Values are angular means ± angular variance, in radians (reported in **Table 3.4**).

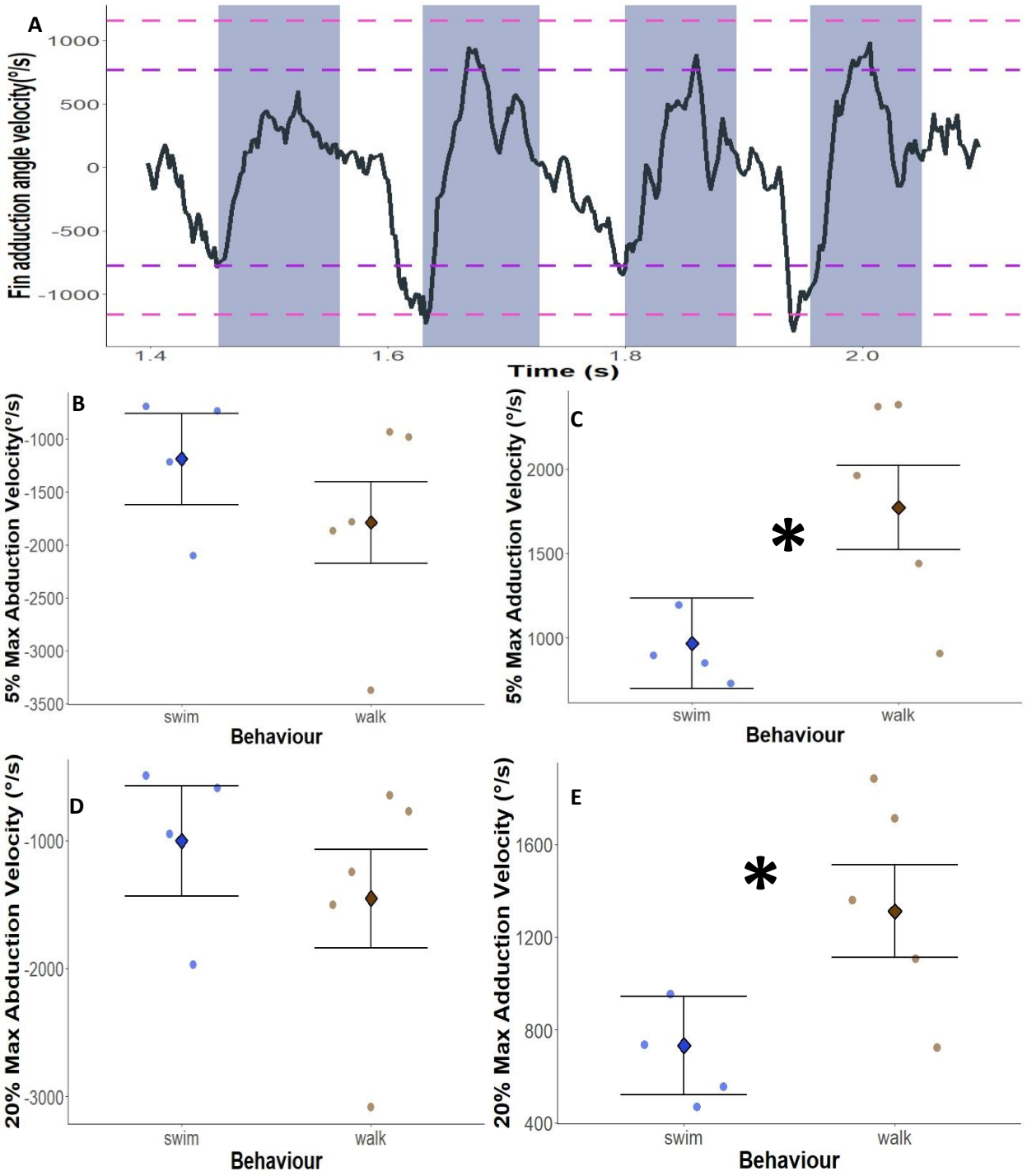

Figure 3.9: Differences in angular velocity of abduction and adduction between swimming and walking at 5% cutoff and 20% cutoff. (A) illustrates the angular velocity of the fin adduction angle at 5% (in pink dotted lines) and 20% cutoffs (in purple dotted lines) from a representative trial, with fin stroke cycles. The shaded and unshaded area is the first and second half of the fin stroke, respectively. The (B) 5% and (D) 20% max abduction velocity are expressed as the angular velocity above the high 5% and 20% cutoff, respectively. The (C) 5% and (E) 20% max adduction velocity

are expressed as the angular velocity below the low 5% and 20% cutoff, respectively. The negative sign indicates fin abduction, and the positive sign indicates fin adduction. All values are presented as emmean ± s.e.m. Points are individuals from the entire data set.

2.3.2 Fin muscle activity during swimming

In the aquatic environment, the adductor muscle was active for a significantly shorter duration than both zono and abductor muscles (**Figure 2.10 A; Table 3.1; Table 3.2**). The zono also had a significantly longer duration than the coraco (**Figure 2.10 A**; **Table 3.2**). The duty factor of the adductor was significantly smaller than all other muscles (**Appendix Figure 1A**; **Table 3.1 & 3.2**). Although the adductor had a higher RIA than other muscles (**Figure 2.10 C**; **Table 3.2**), it was only significantly different from the zono and coraco (**Table 3.1**). The coraco was the only muscle that had a significantly different THRIA than the other muscles during swimming (**Figure 2.10 B**). The coraco reached THRIA significantly later in the fin stroke cycle than all the other fin muscles during swimming (**Figure 2.10 B**; **Table 3.2**). There was no significant difference in burst maximum amplitude across the four fin muscles during swimming (**Figure 2.10 D**; **Table 3.1** & **3.2**).

2.3.3 Fin muscle activity during walking

In a terrestrial environment, adductor muscles turned on significantly longer than the coraco, and zono turned on significantly longer than the abductor (**Figure 2.10 A**; **Table 3.1 & 3.2**). In contrast to swimming, the duty factor of the adductor was significantly larger compared to all other muscles within walking (**Appendix Figure 1A**; **Table 3.1 & 3.2**). Opposed to what was observed in swimming, the adductor had a significantly smaller burst RIA than the rest of the fin muscles (**Figure 2.10 C**; **Table 3.2**). Unlike in swimming, THRIA of all the four fin muscles were not significantly different from each other during walking (**Figure 2.10 B**; **Table 3.1** & **3.2**). As in **Figure 2.10 D**, adductor tended to have a lower maximum amplitude than the other three muscles, but it was only significantly lower than abductor (**Table 3.1** & **Table 3.2**).

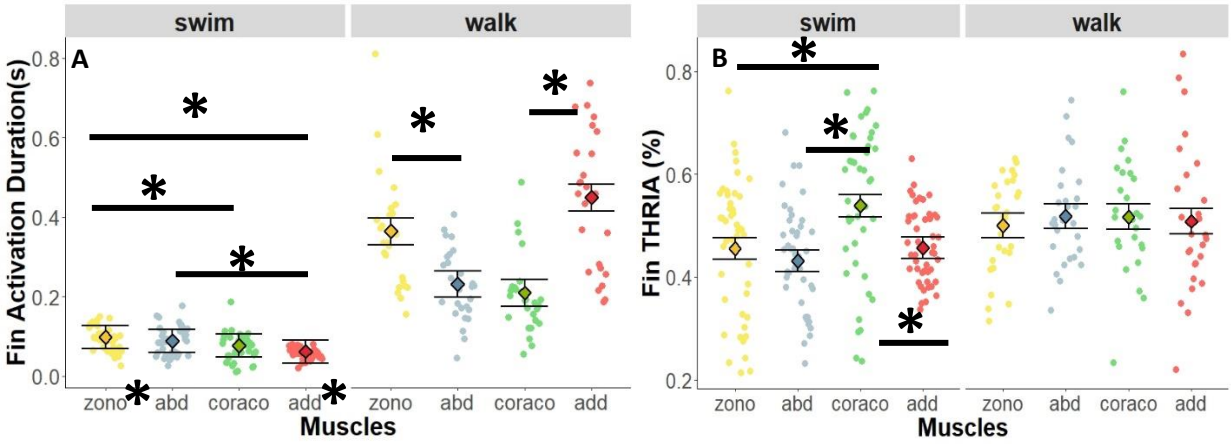

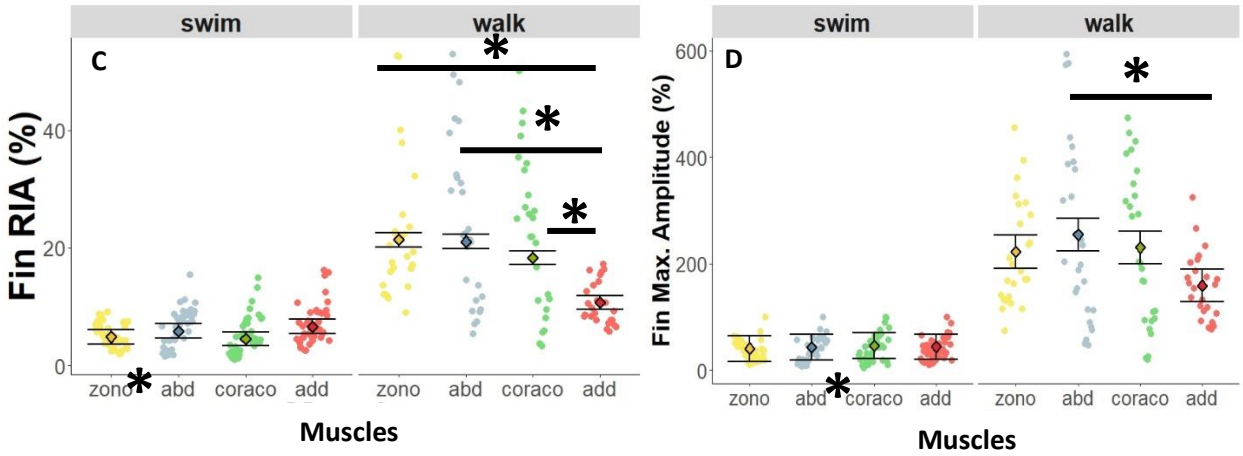

Figure 3.10: Differences in muscle activity of pectoral fin magnitude variables. (A) Activation duration is expressed in seconds. (B) Time to half RIA (THRIA) is expressed as a percentage of activation duration. (C) Rectified integrated area (RIA) of each muscle burst expressed as a percentage of maximum reference burst RIA. (C) Maximum amplitude of each muscle burst is expressed as a percentage of the maximum amplitude observed in a reference trial with steady motion for each individual. All of the values are presented as emmean ± s.e.m. Individual data are the paler shaded dots behind the emmean. The order and colour codes of the muscles listed in the graph corresponds to electrode implantation locations (as in **Figure 2.1**; zono=yellow, abductor=blue, coraco=green, and adductor=red). Asterisks with thin bars indicate significant differences between muscles within each behaviour (swimming and walking). Significances are shown in **Table 3.1**. Asterisks beside muscles on the x-axis label indicate significant differences between swimming and walking for the corresponding muscle (p-values reported in **Table 3.2**).

2.3.4 Fin muscle activity changes from swimming to walking

Both the zono (P=0.0173; **Table 3.2**) and adductor (P=0.00295; **Table 3.2**) turned on significantly longer during walking compared with swimming (**Figure 2.10 A**). As in **Table 3.2**, relative to swimming, the activation duration of the adductor was nearly seven times longer in walking. Additionally, the increase in the duration of the adductor during walking relative to swimming was significantly greater than in the abductor and the coraco (**Figure 2.11 A**). The change in duty factor from swimming to walking was the greatest in adductor muscle (**Appendix Figure 1B**; **Appendix Table 2**). There was no significant change in THRIA for any muscle between swimming and walking (**Figure 2.10 B**; **Table 3.2**). Consequently, the difference of THRIA from swimming to walking was not significantly different across muscles (**Figure 2.11 B**). Compared to swimming, the zono had a significantly greater RIA (P=0.0423) during walking (**Figure 2.10 C**; **Table 3.2**). The increase in RIA of the zono was slightly higher than the other muscles, although the difference in this change was not great enough to be statistically significant (**Figure 2.11 C**). The abductor showed a significant increase in maximum burst amplitude (P=0.0382; **Table 3.2**) in walking relative to swimming (**Figure 2.10 D**). Relative to swimming, while the zono, abductor, and coraco had approximately five times higher maximum amplitude in walking, the adductor had less than four times higher maximum amplitude in walking (**Table 3.2**). But the increases in fin maximum burst amplitude did not significantly differ across the pectoral fin muscles (**Figure 2.11 D**).

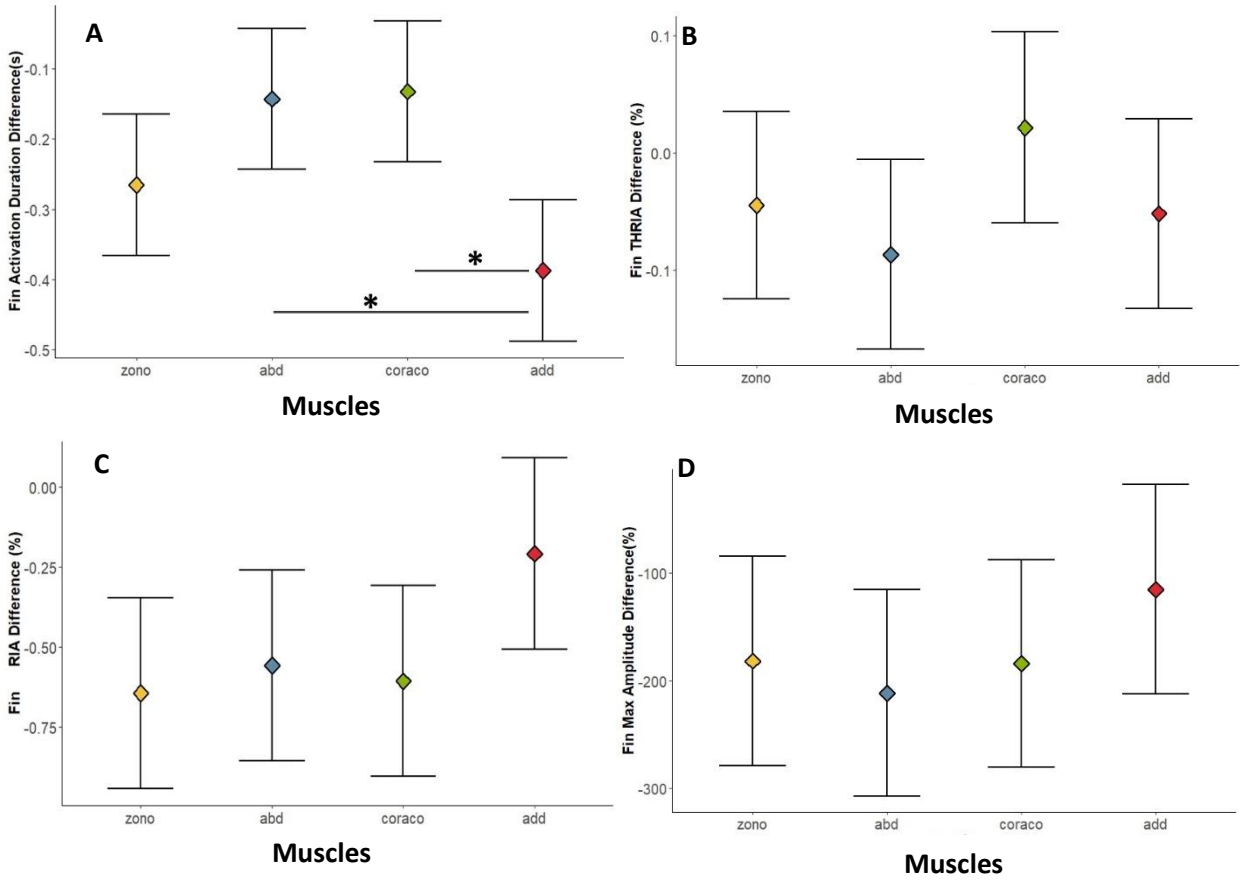

Figure 3.11: Differences between swimming and walking for muscle activity of pectoral fin magnitude variables. The change of (A) activation duration, (B) THRIA, (C) burst RIA, and (D) maximum amplitude from swimming to walking is listed in the same order as the corresponding variables in **Figure 2.10 (A)** to **(D).** All of the values are presented as the contrast of the emmean between swim and walk ± 95% CI (Emmean = estimated marginal means; 95% CI = 95% confidence interval). The order and colour codes of the muscles listed in the graphs corresponds to electrode implantation locations (as in **Figure 2.1**; zono=yellow, abductor=blue, coraco=green, and add=red). Asterisks with thin bars indicate significant differences in the difference between swimming and walking among muscles (**Appendix Table 2**).

2.3.5 Body muscle activity

When swimming, the fish used its anterior body (5) significantly longer than all the other examined parts on the body trunk (**Appendix Figure 3 A**)., and the difference was nearly three times more (**Table 3.2**). In contrast, body (5) generated a significantly smaller burst RIA (**Appendix Figure 3C**), and it was three times less than the remaining body positions (**Table 3.2**). There was no significant difference in THRIA across various body parts (**Appendix Figure 3B**). But at the body (5), the maximum burst amplitude was lower than other body positions, and it was significantly smaller than the body (6), as in **Appendix Figure 3D**. The duty factor of the body (5) was much higher than the rest of the body positions (**Appendix Figure 2A**). There was no significant difference between body (6) and its' opposite side (body (8)) in terms of all measures EMG

magnitude (**Appendix Figure 3 & Figure 2A**), suggesting that the electrode side had no or little influence on muscle activation in water.

During walking, the anterior body (5) turned on significantly longer than the posterior body (7), as in **Table 3.2** (**Appendix Figure 3A**). Body (7) yielded a maximum burst amplitude that was significantly lower than the rest of the body trunk (**Appendix Figure 3D**). Similar to swimming, the shape of individual body muscle burst (THRIA) was not different across positions during walking (**Appendix Figure 3B**). Body (8) had a significantly greater burst RIA than the rest of the body muscle including its' opposite side (**Appendix Figure 3C**). The duty factor showed a significant difference only between body (5) and (7) within walking (**Appendix Figure 2A**).

There was no significant difference detected in activation duration and THRIA of individual body positions between aquatic and terrestrial locomotion. All body positions except for the posterior (body (7)), showed significant increases in burst RIA and maximum amplitude in a walking fish (**Appendix Figure 3C&D; Table 3.2**). Based on **Appendix Figure 4,** and **Appendix Table 2**, the body (8) had greater changes from swimming to walking than the body (7) in THRIA, RIA, and maximum amplitude differences.

2.4 Discussion

2.4.1 Role of the four fin muscles during swimming

During swimming, buoyancy supports the fish passively. *Polypterus* are labriform swimmers using their pectoral fins for thrust production. At slow speeds, body undulations may contribute to stability but are not synchronized with the fins. At higher speeds, the body and pectoral fins coordinate for greater thrust production. In slow swimming fish, all the pectoral fin muscles work in a cyclical order to perform rhythmic fin beats (as described in **Results** and **Figure 2.4 C**). Muscles operate at similar intensities and durations and the adductor appears to work the hardest during the power stroke of the fin.

Zono and abductor dominate during the recovery stroke. All fin muscles operate with the same maximum amplitudes (**Figure 2.10 D**). At the beginning of the fin beat, as in **Figure 2.8 A**, the adductor turns on for the majority of adduction to adduct the fin. Then, the zono activates to elevate the fin for an upstroke of the fin, followed by the activation of abductor which is ready to abduct the fin from the body trunk. After the zono turns off, the coraco turns to lower the fin to reach maximum depression. The zono and coraco work asynchronously for fin elevation and depression, respectively. The adductor and abductor also work independently from each other. The adductor acts for adduction while the abductor acts for abduction, similar in other labroid fishes (Drucker et al., 2005; Drucker & Jensen, 1997). Each pectoral fin muscle plays a distinct role during swimming.

When the zono elevates the fin and the abductor swings the fin forward, they have an extended activation duration relative to the adductor and coraco. Like other labriform swimmers, *Polypterus* propels itself using pectoral fin rowing. During the power stroke, the fin produces thurst, and during the recovery stroke, the fin produces drag (Drucker et al., 2005; Ivanova et al.,

2016; Sfakiotakis et al., 1999). Therefore, to effectively move forward, drag production needs to be minimized during the recovery stroke. As zono and abductor are driving the recovery stroke, they need to be moving slowly, which increases their duration, to decrease the drag produced as the fin abducts into position to start the next power stroke. Since the maximum amplitude of the zono is not different than the others (**Figure 2.10 D)**, the relatively smaller burst RIA of the zono could be contributed by the longer activation duration. Interestingly, the coraco muscle is the only muscle with a significantly longer THRIA suggesting it turns on in a more gradual way, possibly providing a stabilizing depression, or reducing the possibility of producing inopportune drag. The maximum amplitudes of all muscles are achieved at the same level, which could be caused by the cyclical activation pattern. Since all the muscles turn on one by one, the force required for thrust could be evenly contributed by each muscle throughout the entire fin stroke.

2.4.2 Role of the four fin muscles during walking

During walking, the fish face terrestrial loading due to gravity. This new loading regime changes the forces the animal must overcome to move forward. Our data suggest that pectoral fin muscle activation patterns become more variable and generally higher in magnitude compared to swimming. In humans, the white muscle has a high activation threshold and larger motor units (one nerve innervates a greater number of muscle fibers than red muscle fiber) (Radák, 2018), implying that usage of white muscle essentially yields greater muscle signal intensity. The increase in muscle activity shown in walking fish could reflect greater white muscle recruitment in the terrestrial environment. There are large differences in activation duration for each of the muscles with the zono and adductor muscle activated for a much longer portion of each stroke during walking than during swimming (**Figure 2.10 A & 2.8 B**). Although previous studies showed that the adductor muscles suffered the most damage after walking, the RIA of the adductor in this study was lower than the other pectoral fin muscles and its max amplitude was less than that of the abductor. The damage to the adductor is not necessarily caused by a more explosive use of a muscle but can be explained by a change in activation timing. Different from swimming, during walking, the adductor works synchronously with the zono, and the coraco during the power stroke, and synchronously with the abductor during the recovery stroke. Because the adductor is active during both fin stance and swing, it may have little time for recovery between strokes, leading to fatigue and possible injury. During the stance phase (the first half of fin stroke cycle in **Figure 2.8 B**), the adductor is likely primarily responsible for adducting the fin. The activation of the abductor and coraco during the start of stance (**Figure 2.8 B**) could stiffen the pectoral fin when contracting against the antagonist muscle (adductor). To stabilize the fin step, the abductor may need to exert more forceful contraction, which could require higher maximum burst amplitude, to pinch/load the fin onto the ground. Also, the abductor has an increased RIA, suggesting a greater muscle effort is required for weight-bearing due to gravity (Standen et al., 2016). While the abductor and adductor contract against each other, the coraco is active likely for rotating the fin downwards for supination onto the ground (Wilhelm et al., 2015), as well as pulling the fin backward. Both the adductor and zono turn on together during the fin swing of the step (**Figure 2.8 B**). While the zono activates for swinging the fin over to the front and

reaching maximum fin elevation, the adductor possibly plays a role in holding the fin in shape as well as governing the swing speed. As opposed to what was seen in swimming, the muscle effort (burst RIA) of the adductor becomes smaller than the other muscles, which could be contributed by the greater activation duration and lower maximum amplitude. At the middle of the stance phase of the right pectoral fin (**Figure 2.8 B**), the fish head falls down and continues moving towards the right, which often occurs at a resting period where all the pectoral fin muscles are turned off. This indicates that during walking, fin muscles are shut off to relax during free-falling of the fish head. The change in muscle activity was not only found in the pectoral fin but also in the body trunk. The mid-body trunk had greater muscle effort (maximum amplitude and burst RIA) compared to the posterior body during walking (**Appendix Figure 3C&D; Table 3.2**), which agrees with the previous observation of body muscle activity (Foster et al., 2018).

2.4.3 Fin muscles switch roles from swimming to walking

2.4.3.1 Prolonged and unaccustomed exercise, and muscle damage

When comparing muscle activation and kinematics between swimming and walking, there were changes seen in the role of the adductor muscle. Minimum adduction is significantly greater during walking. When the fin is maximally abducted and pulled closer to the body, the adductor is anatomically lengthened to a greater extent than normal swimming (**Figure 2.1**). During walking, the adductor remains active as it is stretched (**Figure 2.6 B**), suggesting that the adductor possibly sustains eccentric contraction during the latter period of activation. Additionally, the adductor is used for a longer duration during walking than other muscles. Although Foster et al. (2018) suggests that the adductor produces double bursts within a stroke when walking, the data in this study suggest that the adductor is active through most of the fin stroke (**Figure 2.8 B**) with relatively weak and variable signal intensity (**Figure 2.10 C & D**). The adductor sustains contraction for two kinematic performances (stance and swing). Consequently, there is little time for the adductor to recover between fin steps, which could ultimately fatigue the muscle and could cause damage. Muscle fatigue is often linked to muscle strain in human (Del Coso et al., 2012; Shekarchizadeh et al., 2018). Lack of recovery time and possible eccentric contraction could be crucial to walking-induced damage of the adductor.

In contrast, during swimming, the adductor turns on for a shorter time with greater muscle output and stronger muscle activity compared to the other muscles. The adductor muscle stays active only for the first ¾ of adduction with the aid of the activation of the zono. Additionally, the adductor activation timing changes from being involved in one function (adduction) in water to two functions on land. When on land, the adductor acts to: (1) bring the fin towards the body (with the activation of the coraco) during the stance phase, and (2) bend and hold the fin in shape (when zono swings the fin forward) during the swing phase. The mode of how the adductor works regularly in swimming is completely changed when the fish is placed on the land. Although the fish is capable of showing behavioral plasticity in response to terrestrial acclimation (Standen et al., 2014, 2016), it requires a dramatic change in muscle usage so the animal can perform a behaviour that it is likely not specialized for. Consequently, the adductor could have temporary

exercise-induced muscle damage by this unaccustomed terrestrial exercise, like muscle damage after unaccustomed exercises reported in humans (Del Coso et al., 2012; Hunter et al., 2012). Although this is a plausible explanation for damage in the adductor muscle, the zono muscle also operates with an extended activation duration during walking but did not show any significant damage in the previous study (Dhuper, 2018). I hypothesize that during walking, the zono is never in direct contact with the ground. Therefore, the zono does not suffer from ground reaction force, which may prevent excessive damage. In addition, the fish does not tend to depress or elevate the fin more during fin strokes on land than in water (**Figure 2.7 F & G**). This hints that the zono is likely not being stretched beyond its natural range in this novel walking exercise. The zono possibly undergoes concentric contraction during the early swing phase and experiences less change in external muscle length between behaviours relative to the adductor. Thus, the zono is less likely to experience abundant muscle fiber damage than the adductor.

2.4.3.2 Mechanical advantages in a lever system and muscle fiber type transition

Both the 5% and 20% maximum adduction velocity increases in walking compared with swimming (**Figure 2.6**), implying that fins are adducted faster on land. In addition, maximum adduction velocity often occurs during fin stance on land (**Figure 2.6 A**). In the terrestrial environment (**Figure 2.8 B**), the abductor, coraco, and adductor are active together to facilitate fin movement speed during fin stance. White muscle fibers are recruited for fast contraction to produce speed movement (Jayne & Lauder, 1994). The sudden increase in fin velocities during walking adduction likely requires white muscle fiber recruitment for effectively reaching the faster adduction speed. In addition, since this rapid motion occurs during stance when the fin experiences a large load, it is possible that higher force is required to bear the load on land. Thus, the potential need for increased speed and force for accomplishing the terrestrial locomotion could eventually lead red muscle fibers to transition to white muscle fibers over an extended course on land.

During stance in this dataset, the lateral side of the fin (where the abductor is located) is flipped on the ground (**Figure 2.12 A**) which follows a gait IIa walking pattern (**Appendix Figure 6**) as described by Standen et al. (2016). At the beginning of the stance, the abductor contracts to secure the fin on the ground, which results in a ground reaction force applied back on the fin. In this study, it is likely that the load on the fin should be located at the center of the pressure of the partial fin that is in contact with the ground. For ease of presentation, I assumed that the load is concentrated at the most proximal portion of the fin that is on the ground. As the abductor, coraco, and adductor contract to supply effort for fin motion, the pectoral girdle joint potentially works as a fulcrum (**Figure 2.12**), like the human elbow. Both abductor and coraco contain two individual muscles (**Appendix Figure 5**) with potentially varied muscle lengths due to the different insertion and origin positions. As in **Figure 2.12 B & D**, the abd. sup. and the scapulocoracoid could work as a class III lever to quickly flip the pectoral fin onto the ground for initiation of stance. Working as a class III lever is beneficial for allowing small changes in muscle length to produce large excursions at the fin tip (Davidovits, 2013), helping facilitate speed. Because the abd. sup. attaches close to the load in these fish, there is no force mechanical advantage suggesting

muscles must produce large forces during walking. The abd. sup. may require more endurance as it is required to keep the fin on the ground throughout stance. On the other hand, the abd. pro. is more distally inserted on the joint (**Figure 2.12 B**). When abd. pro. contracts to produce force onto the ground (**Figure 2.12 E**), it creates an effort arm that is longer than the loading arm, yielding a class II lever. Intrinsically, this abd. pro. muscle has a mechanical advantage and so the muscle does not need to produce as much force. The different positions of muscles in the fin and their resulting mechanical advantage suggests a need for high force production and speed proximally with lower force production and endurance distally which is supported by the muscle fiber remodeling data that shows a larger transition to white fibers proximally (Du & Standen, 2017). Overall, it appears that the abd. sup. muscle maintains the speed advantage while the abd. pro. muscle maintains a force advantage, both parts of the muscle working together to maintain an overall functional advantage. Therefore, in conjugation with the increasing white muscle fiber from distal to proximal in abductor (Du & Standen, 2017), while the abd. pro. is overseeing force production, the abd. sup. is maintaining speed performance. Similar to the abductor muscles, the coraco muscles with different lengths (**Figure 2.12 F & G**), which are coraco II and coraco I, work as class III, and class II levers, respectively (**Figure 2.12 H & I**). The coraco muscles contract to pull the fin toward the body and down to the ground, which aids the act of loading the fin onto the ground by the abductor. (**Figure 2.12 F & H**). As the short coraco II muscle contracts, it yields an effort between the load and the joint (fulcrum), which results in a class III lever (**Figure 2.12 H**). Since the effort arm in coraco II has a shorter arm than the loading arm, the coraco II muscle generates large fin tip excursions with a small change in muscle length, which is beneficial in facilitating speed when pulling the fin towards the body. To further increase the production of speed, it would be preferable to use white muscle fiber for fast contraction (Jayne & Lauder, 1994). If the higher fin motion speed is consistently required over a long-term walking, this may lead to a muscle fiber type switch to white muscle fiber at the proximal portion as in fish with terrestrial acclimation (Du & Standen, 2017). Whereas, the long muscle, coraco I (**Figure 2.12 G & I**) works as a class II lever with a mechanical advantage suited for generating force, similar to the abd. pro. muscle. Due to this mechanical advantage, coraco I may need less force to bring the fin down and resist the loading from the contrasting abductor, which prevents the abductors from flipping away from the body and securing the fin stance. Thus, coraco has less white muscle fiber but more red muscle fiber on the distal end as seen in the study on long-term walking fish (Du & Standen, 2017), which allows for some amount of force production and the ability for the muscle to endure the loading on the fin. As discussed, the two abductors and coraco muscles with different lengths work together as a whole during stance to provide fin motion speed, muscle strength, and endurance. During stance, the adductor is likely working as a class II lever with the extended insertion on the fin rays from the pectoral joint (fulcrum) (**Figure 2.13 A & B**). As the adductor is active throughout the majority of stance, it could be working in conjunction with the coraco muscles to ensure the positioning of the fin and maintain line of action for the abductor muscles into the ground, which may help prevent the fin from moving away from the body. Most likely, when the ventral portion of the adductor is active and pulls from the head

originating on the medial surface of the scapulocoracoid, the fin is then pulled back towards the body (**Figure 2.13**).

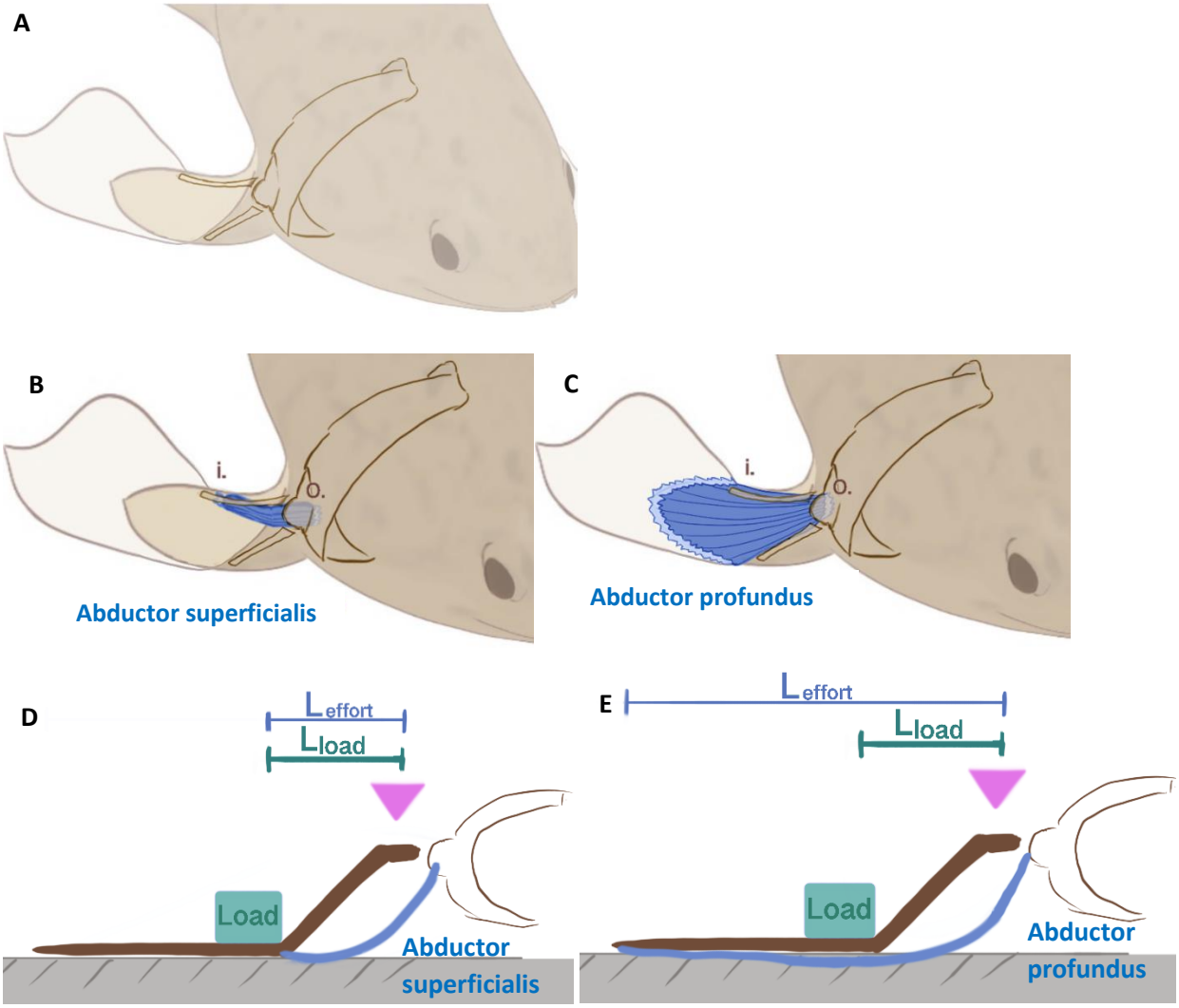

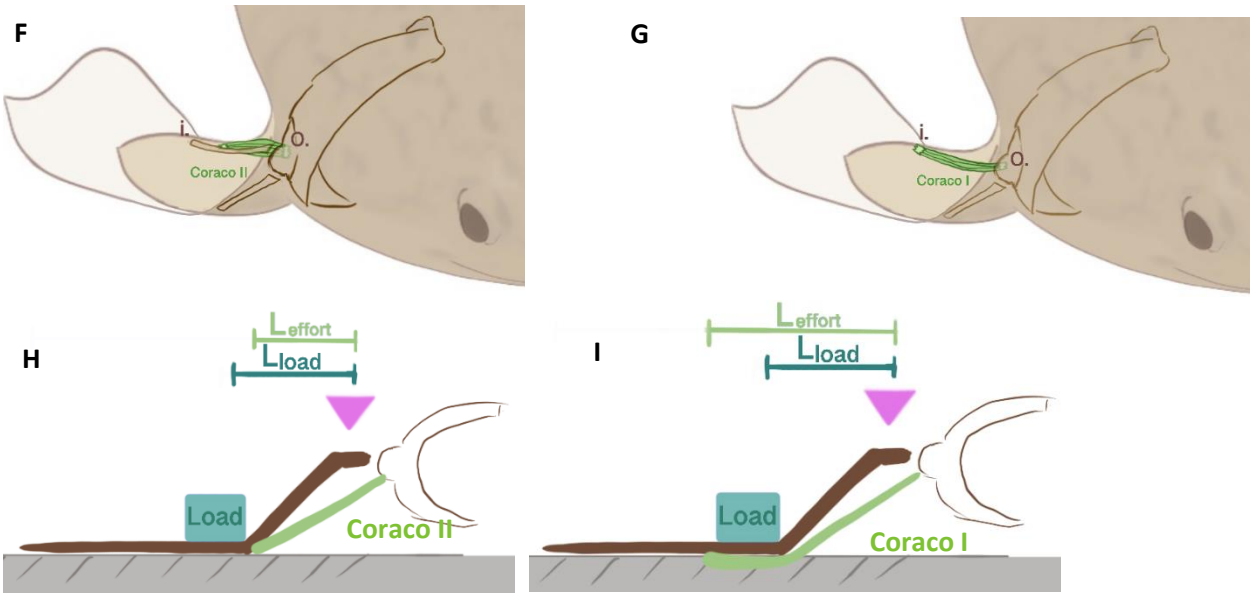

Figure 3.12: Schematic lever system in pectoral fin musculature during stance phase of walking. (A) Placement of the pectoral girdle and fin bones in a walking fish. Abd. sup. ((B) and (D)) and abd. pro. ((C) and (E)) are coloured in blue. Coraco II ((F) and (H)) and coraco I ((G) and (I)) are coloured in green. The load is indicated as the most proximal point of contact of the fin with the ground with loading arm as L_{load}. The effort arm of each muscle is demonstrated in a lever system based on the insertion and origin in (D), (E), (H), and (I), as L_{effort}. A purple triangle indicates the pectoral joint as a theoretical fulcrum in the system. Insertion (i.) and origin (o.) of each muscle are indicated in (B), (C), (F), and (G). The pectoral fin is presented as the medial side of the fin facing up. The anatomy is consistent with Figure 2.1 and based on the study by Wilhelm et al. (2015).

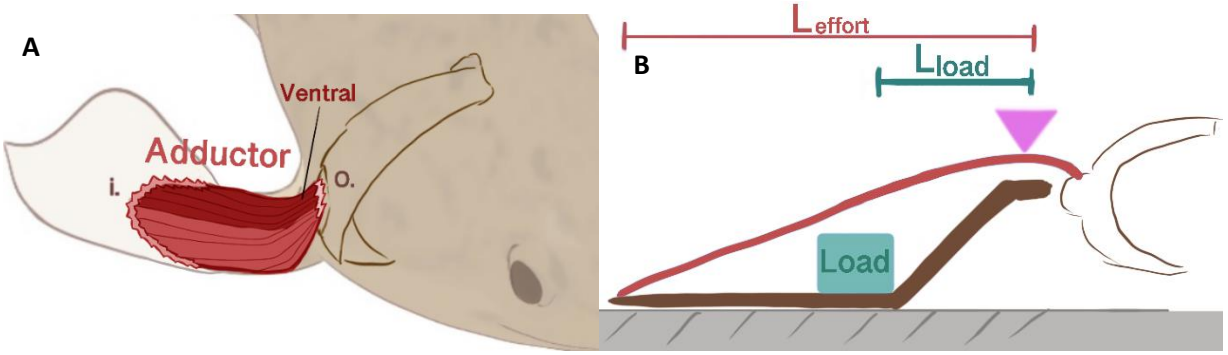

Figure 3.13: Schematic lever system of adductor during stance phase of walking. (A) muscle position of adductor is demonstrated during fin plant. The load is indicated as the most proximal point of contact of the fin with the ground with loading arm as L_{load}. The effort arm of adductoris demonstrated in a lever system based on the insertion and origin in (B), as L_{effort}. The purple triangle indicates the pectoral joint as a theoretical fulcrum in the system. Insertion (i.) and origin

(o.) of each muscle are indicated. The illustrations are presented in the same manner as **Figure 2.12**. The anatomy is consistent with **Figure 2.1** and based on the study by Wilhelm et al. (2015).

During the swing phase of the fin stroke, it could be assumed that the load on the pectoral fin is represented by the center of the fin mass when the fin is off the ground. The adductor as a whole still works as a class II lever (**Figure 2.14 B & D**), however, the dorsal portion may be preferentially activated (pulling from the dorso-medial scapulocoracoid), which could bend the fin and hold it in shape (**Figure 2.14 B**). During walking, the adductor likely produces asymmetric pulls by activating the two different heads of the adductor, which results in the constant activation with highly variable activation signals (**Figure 2.4 C & D**). Since the electrodes were placed in the middle of the adductor, it yields a weaker signal that is constantly on. The variation of muscle activity that was seen between individuals could be due to electrode placement. In conjunction with the adductor, the zono could bring the fin up and forward for abduction during the fin swing. Contracting the zono about the scapulocoracoid (fulcrum) to supply effort for fin motion along with the loading by the fin weight, could yield a class III lever (**Figure 2.14 C & E**). Consequently, when the zono primarily facilitates forward fin motion, this muscle is at a mechanical disadvantage, particularly, in force. With the short effort arm, zono may need a greater muscle effort to resist the load, which is reflected by the increased muscle activation duration and burst RIA (**Figure 2.10 A & C**). Essentially, the required increased muscle effort and higher force could favor the shift to white muscle fibers after terrestrial acclimation. What's fascinating is that the adductor in a swimming context has a singular and sensical function of adduction. When the muscle is used in a novel environment, the adductor in conjunction with other muscles moves the fin with a completely different motion, which is an opposite kinematic effect than in swimming motion. Such a dramatic switch in function and unaccustomed exercise could possibly explain why the adductor muscle is greatly damaged after walking (Dhuper, 2018).

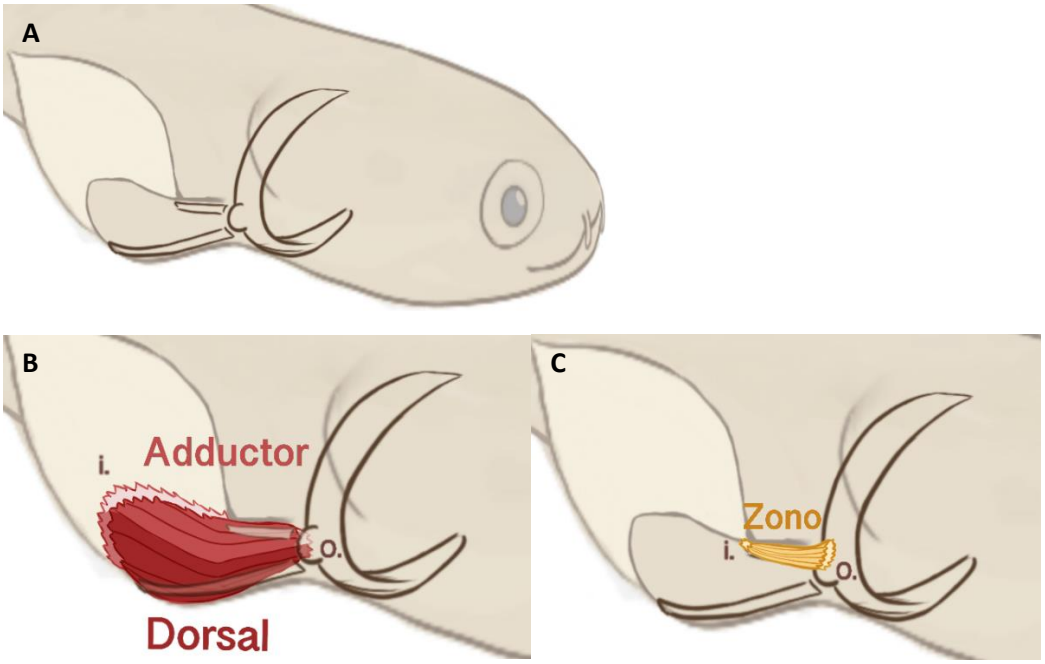

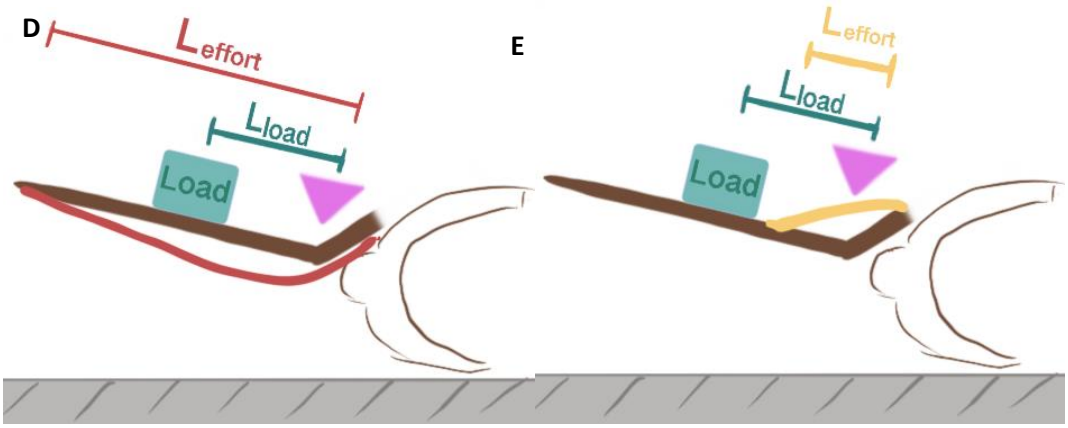

Figure 3.14: Schematic lever system in pectoral fin musculature during swing phase of walking. (A) Placement of the pectoral girdle and fin bones with the lateral/outside of fin facing outward. The adductor ((B) and (D)) is coloured in red. Zono ((C) and (E)) are coloured in yellow. The load is indicated as the center of the mass of the fin with loading arm as Lload. The effort arm of each muscle is demonstrated in a lever system based on the insertion and origin in (D) and (E), as Leffort. The purple triangle indicates the pectoral joint as a theoretical fulcrum in the system. Insertion (i.) and origin (o.) of each muscle are indicated in (B) and (C). The anatomy is consistent with Figure 2.1 and based on the study by Wilhelm et al. (2015).

2.5 Conclusions

The kinematic and muscle activity data collected from *Polypterus* indicate a change in the role of the pectoral fin musculature from swimming to walking. Although the shapes of muscle activation bursts were similar between the two behaviours, muscle effort increased during walking as measured by EMG magnitude. In addition, antagonistic muscles were more likely to be on simultaneously during walking, leading to an eccentric contraction in the adductor muscle. Adductor muscles also remained active for the entire stroke cycle during walking and thus operated at much longer muscle lengths and with less opportunity to rest than during swimming. Differences in insertion and origin of different muscles change the mechanical advantage of individual muscle groups, impacting their need to produce higher forces during novel locomotory modes. This study demonstrates that: (1) damage found in adductor muscle in previous studies can be explained by the extended activation duration, by eccentric contraction due to muscle length during activation, and by antagonistic co-contraction of the abductor and coraco muscles; (2) increased need for acceleration and force production during walking provides mechanisms for eliciting a transition to glycolytic muscle fibers found in terrestrially acclimated fishes. Although these data cannot explain the evolutionary changes that may have taken place during the fin to limb transition, they do provide walking-induced mechanisms that contribute to the plasticity that has been suggested to influence the morphological changes seen in the fossil record.2.6 Tables

2.6.1 EMG Variables

Table 3.1: Connecting letter reports based on Bonferroni-corrected p-values for EMG variables across fin muscles and body position, within a given behaviour.

Fin Variables	**Behaviour**	**Fin muscles**			
		zono	**Abductor**	**coraco**	**Adductor**
Activation Duration	Swim	a	ab	bc	c
	walk	A	B	B	A
THRIA (% activation duration)	Swim	a	a	b	a
	walk	A	A	A	A
RIA (% max. RIA)	Swim	a	ab	a	b
	walk	A	A	A	B
Max. Amp. (% max. amp.)	Swim	a	a	a	a
	walk	AB	A	AB	B
Duty Factor (% activation duration)	Swim	a	ab	bc	c
	walk	A	B	B	C
Body Variables	**Behaviour**	**Body Positions**			
		Body (5)	**Body (6)**	**Body (7)**	**Body (8)**
Activation Duration	Swim	a	b	b	b
	walk	A	AB	B	AB
THRIA (% activation duration)	Swim	a	a	a	a
	walk	AB	A	B	A
RIA (% max. RIA)	Swim	a	b	b	b
	walk	A	A	A	B
Max. Amp. (% max. amp.)	Swim	a	b	ab	ab
	walk	A	A	B	A

Duty Factor (% activation duration)	Swim	a	b	b	b
	walk	A	AB	B	AB

The EMG variables from the four fin muscles and four body positions are arranged as in the top and bottom part of the table. Estimated marginal means and their standard errors are listed in Table 3.2. Each alphabetic letter represents a statistically different mean. Lower-case letters, and upper-case letters indicate the differences across fin muscle or body position within swimming, and walking behaviour, respectively.

Table 3.2: Results of mixed-model ANOVAs of fin and body EMG variables between behaviours.

Fin Variables	Fin muscle	behaviour		ANOVA P-value	Bonferroni-corrected P-value	F – value (d.f.)
		swim	walk			
Activation duration ± s.e.m. (s)	Zono	0.0989±0.0290 ^{a}	0.3643±0.0340 ^{A}	0.0011	0.01743*	45.44953 (1,5)
	abductor	0.0886±0.0290 ^{ab}	0.2316±0.0335 ^{B}	0.0144	0.23012	
	Coraco	0.0770±0.0290 ^{bc}	0.2095±0.0335 ^{B}	0.0193	0.30836	
	adductor	0.0625±0.0290 ^{c}	0.4497±0.0341 ^{A}	0.0002	0.00295*	
THRIA ± s.e.m. (% activation duration)	Zono	0.455±0.0212^{a}	0.500±0.0239^{A}	0.2084	1.000	2.0844 (1,5)
	abductor	0.432±0.0213^{a}	0.519±0.0242^{A}	0.0397	0.635	
	Coraco	0.538±0.0216^{b}	0.517±0.0242^{A}	0.5317	1.000	
	adductor	0.456±0.0209^{a}	0.508±0.0246^{A}	0.1595	1.000	
RIA ± s.e.m. (% max RIA)	Zono	4.84±1.21^{a}	21.4±1.20^{A}	0.0026	0.0423*	30.60799 (1,5)
	abductor	5.83± 1.21^{ab}	21.1±1.20^{A}	0.0048	0.0775	
	Coraco	4.53± 1.21^{a}	18.3±1.20^{A}	0.0034	0.0547	

	adductor	6.63± 1.21[b]	10.7±1.20[B]	0.1346	1.000	
Max Amp ± s.e.m. (% max burst amplitude)	Zono	40.7±24.1[a]	222.5±31.0[AB]	0.0049	0.0782	23.033831 (1,5)
	abductor	42.9±241.[a]	224.6±30.4[A]	0.0024	0.0382*	
	Coraco	46.1±24.2[a]	230.3±30.4[AB]	0.0044	0.0704	
	adductor	43.6±24.1[a]	158.9±31.0[B]	0.0286	0.4580	
Duty Factor ± s.e.m. (% activation duration)	Zono	0.552±0.0388[a]	0.582±0.0462[A]	0.6446	1.000	0.24057 (1,5)
	abductor	0.491±0.0388[ab]	0.422±0.0454[B]	0.3010	1.000	
	Coraco	0.436±0.0396[bc]	0.375±0.0462[B]	0.3614	1.000	
	adductor	0.349±0.0384[c]	0.746±0.0462[C]	0.0012	0.0192*	
Body Variable	**Body position**	**behaviour**		**ANOVA P-value**	**Bonferroni-corrected P-value**	**F – value (d.f.)**
		swim	**walk**			
Activation duration ± s.e.m.	Body (5)	0.300±0.0417[a]	0.227±0.0288[A]	0.0851	1	4.58766 (1,5)
	Body (6)	0.114±0.0443[b]	0.201±0.0288[AB]	0.0686	1	
	Body (7)	0.126±0.0443[b]	0.178±0.0288[B]	0.2196	1	
	Body (8)	0.146±0.0417[b]	0.214±0.0288[AB]	0.0998	1	
THRIA ± s.e.m. (% activation duration)	Body (5)	0.509±0.0357[a]	0.533±0.0301[AB]	0.4113	1.00	0.80278 (1,5)
	Body (6)	0.485±0.0381[a]	0.583± 0.0301[A]	0.0214	0.3429	
	Body (7)	0.513±0.0352[a]	0.500±0.0302[B]	0.6516	1.00	
	Body (8)	0.437±0.0352[a]	0.562±0.0301[A]	0.0049	0.0782	
	Body (5)	1.24±0.906[a]	52.44±8.062[A]	0.0014	0.02258*	

RIA ± s.e.m. (% maximum RIA)	Body (6)	4.81± 0.933[b]	52.63±8.062[A]	0.0019	0.03073*	17.197584 (1,5)
	Body (7)	3.78±0.933[b]	20.28±8.062[A]	0.0953	1.000	
	Body (8)	3.93±0.906[b]	93.47±8.062[B]	0.0001	0.00163*	
Max Amp ± s.e.m. (% maximum burst amplitude)	Body (5)	10.0±6.75[a]	439.3±51.58[A]	0.0004	0.0065*	69.49607 (1,5)
	Body (6)	38.1±7.05[b]	415.7±51.58[A]	0.0007	0.0119*	
	Body (7)	23.9±7.05[ab]	162.4±51.58[B]	0.0435	0.6955	
	Body (8)	26.3±6.75[ab]	535.0±51.58[A]	0.0002	0.0029*	
Duty Factor ± s.e.m. (% activation duration)	Body (5)	0.657±0.0658[a]	0.408±0.0281[A]	0.0178	0.285	0.0178 (1,5)
	Body (6)	0.262±0.0734[b]	0.353±0.0283[AB]	0.3025	1.000	
	Body (7)	0.260±0.0629[b]	0.337±0.0281[B]	0.3139	1.000	
	Body (8)	0.290±0.0629[b]	0.375±0.0281[AB]	0.2730	1.000	

The EMG variables from the four fin muscles and four body positions are arranged as in the top and bottom part of the table. Connecting letters are in superscript following the standard errors. Each trial is nested in the corresponding fish, and individual fish is coded as a random factor in the models. An asterisk indicates a significant difference between behaviours within a designated muscle. The asterisks are assigned based on the Bonferroni-corrected adjusted p-values. Numerator and denominator d.f. (degree of freedom) are given in parentheses after F-values.

2.6.2 Kine Variables

Table 3.3: Results of mixed-model ANOVAs of kinematic variables between behaviours

Variables	Behaviour		ANOVA p-value	F-value (d.f.)
	swim	walk		
Elevation range ± s.e.m. (mm)	2.06 ± 0.297	4.15 ± 0.351	0.0061*	20.70708 (1,5)
Maximum elevation ± s.e.m. (mm)	-5.53 ± 0.706	-4.15 ± 0.653	0.2112	2.05416 (1,5)

Minimum elevation ± s.e.m. (mm)	-7.59 ± 0.591	-8.43 ± 0.544	0.3471	1.0763 (1,5)
Adduction angle range ± s.e.m. (°)	21.9 ± 8.26	67.4 ± 7.91	0.0024*	32.07178 (1,5)
Maximum adduction ± s.e.m. (°)	202 ± 10.6	210 ± 10.6	0.1199	3.5083 (1,5)
Maximum abduction ± s.e.m. (°)	180 ± 15.1	143 ± 14.8	0.0084*	17.73999 (1,5)
5% max. abduction velocity ± s.e.m. (°/s)	-1189 ± 430	-1789 ± 385	0.3459	1.081952 (1,5)
5% max. adduction velocity ± s.e.m. (°/s)	967 ± 268	1172 ± 248	0.0463*	6.934335 (1,5)
20% max. abduction velocity ± s.e.m. (°/s)	-1004 ± 430	-1453 ± 385	0.4716	0.605623 (1,5)
20% max. adduction velocity ± s.e.m. (°/s)	733 ± 212	1312 ± 199	0.0434*	7.228027 (1,5)

Each kinematic variable is compared between swimming and walking. Each trial is nested in the corresponding fish, and individual fish is coded as a random factor in the models. Asterisks represent for significant differences. Numerator and denominator d.f. (degree of freedom) are given in parentheses after F-values.

2.6.3 Temporal Variables

Table 3.4: Directionality of EMG and kinematic temporal variables

EMG temporal variables							
variable	**muscle**	**Behaviour**					
		Swim (mean ± variance)	**Rayleigh P-value**	**H-R P-value**	**Walk (mean ± variance)**	**Rayleigh P-value**	**H-R P-value**
onset	Zono	0.8205±0.9119	-	<0.001*	2.5348±0.3162	-	<0.001*
	Abductor	-2.6261±0.3745	<0.001*	-	-0.7372±0.2777	-	<0.001*

	Coraco	-1.5548±0.8506	<0.001*	-	-0.6814±0.2368	-	<0.001*
	adductor	0.1242±0.3804	-	<0.001*	2.8734±0.6233	-	<0.001*
offset	Zono	-1.8956±0.7064	<0.001*	-	0.0375±0.4298	<0.001*	-
	Abductor	-0.3617±1.1675	<0.001*	-	1.7625±0.6521	-	<0.001*
	Coraco	1.3614±0.6612	<0.001*	-	1.5254±0.2914	-	<0.001*
	adductor	2.3096±0.2809	<0.001*	-	1.3176±1.4881	-	<0.001*
Kinematic temporal variables							
variable	**Body part**	**Behaviour**					
		Swim (mean ± variance)	**Rayleigh P-value**	**H-R P-value**	**Walk (mean ± variance)**	**Rayleigh P-value**	**H-R P-value**
Max. adduction	**Pectoral fin**	-2.3898±1.1643	0.002*	-	-2.7273±0.3069	<0.001*	-
Min. adduction		0.9776±0.9936	<0.001*	-	0.8802±0.3873	-	<0.001*
Max. elevation		-1.9846±0.5121	<0.001*	-	-2.2255±1.2055	0.034*	-
Min. elevation		0.9977±0.7180	<0.001*	-	-0.3287±1.8275	0.86	-
Max. elevation	**nose**	-	-	-	0.8123±0.2833	<0.001*	-

Min. elevation		-	-	-	2.0870±0.3476	<0.001*	-

The values of all variables are shown as angular mean ± angular variance, in radians. Asterisks under p-value indicate significant directionality (P>0.05) in relation to fin strokes. The variables that had an equal variation and did not differ from a von Mises distribution (Kuiper test, P>0.05) were tested by Rayleigh's test for directionality. The rest of the variables that failed the assumptions above were tested by Hermans-Rasson test for directionality. H-R stands for Hermans-Rasson.

Table 3.5: Results of Watson-Williams multi-sample tests of EMG and kinematic timings between behaviours

variables	position	Watson-Williams P-value	Watson-wheeler P-value
Onset	Zono	-	0.001*
	Abductor	-	0.001*
	Coraco	-	0.001*
	abductor	-	0.001*
Offset	Zono	<0.001*	-
	Abductor	-	0.001*
	Coraco	-	0.01*
	abductor	-	0.001*
Max adduction	Fin	0.2423	-
Min adduction	Fin	-	0.5
Elevation max	Fin	-	0.005*
Elevation min	fin	0.0827	-

Asterisks indicate significances when P<0.05. The parametric Watson-Williams tests were only performed when data are directional (see Table 3.5) and obey a von Mises distribution (Kuiper test, P>0.05) for both behaviours. The nonparametric Watson-Wheeler tests were performed on the rest of the data.

Chapter 3. Future directions

In this investigation, different aquatically raised individuals were released to swim and walk for approximately 10 fin beats to see the changes that occur when fish first walk on land. Particularly, the instantaneous change in pectoral fin muscle activity and kinematic performance was evaluated between the two behaviours. Data in this study have suggested that there was an immediate change in muscle activation pattern in the pectoral fin in response to acute walking. It was found that the fin muscles activated at different times of the fin stroke cycle and played different roles between behaviours. In a previous study, *Polypterus* changes muscle fiber type from red to white after being raised on land for extended periods of time. Although this study only looked at the instantaneous changes, those changes can explain the plastic response after terrestrial acclimation. This study showed increased muscle effort and faster fin adduction (faster muscle contraction) in the pectoral fin when fish first walked on land. Such changes may push muscle fiber composition towards white muscle fibers. In addition, muscles are not afforded any mechanical advantage during walking, so a greater amount of force, potentially powered by more white muscle fibers, should be required. If those needs are required consistently throughout long term terrestrial acclimation, it would eventually lead to the plastic responses seen in terrestrially raised fish. Given the plasticity responses in morphology and behaviour induced by walking, *Polypterus* has been a remarkable model to help understand the evolutionary fin-to-limb transition. In this study, I have studied the kinematics and fin muscle activation of all pectoral fin muscle groups during swimming and short-term walking, which indicated some possible causes of muscle damage induced by short-term walking, and the potential driving mechanisms that lead to muscle fiber phenotypic change after terrestrial acclimation.

This study suggested that the adductor experienced unaccustomed sustained exercise with little rest which could lead to fatigue and muscle damage. As muscles fatigue, their force and power output drop (Vøllestad, 1997). Although *Polypterus* fin muscles are too small for current techniques (fluoromicrometry), in the future, we would dream of measuring muscle length change and activation level as fish are exercised to exhaustion on land. Then, we could measure the muscle force and power output of the pectoral fin from the beginning, the middle, and the end of the exercise. Specifically, it would be expected that both force and power output would decrease over time as an indication of muscle fatigue. We could also measure muscle chemistry, looking at metabolic products such as lactic acid to gain insight into what limits the performance of fishes during terrestrial forays.

In this current study the adductor experienced sustained eccentric contraction during walking as it was active when the fin was maximally abducted. The muscle undergoing concentric contraction would mean that muscle shortens to produce force, and the muscle undergoing eccentric contraction would mean that muscle is active when it is stretched by the antagonistic muscle. Consequently, the muscle is more prone to injury and damage when it is overstretched (Morgan et al., 1999). The adductor muscle did not have a distinct muscle burst, but rather constantly turned on with a low amplitude and occasional higher amplitude throughout the

muscle activation. We would like to know the limitation of individual muscle length and whether the muscles exceed this limit during terrestrial locomotion. Unfortunately, due to the limitation of technology nowadays, we are yet unable to measure the change in muscle length in the pectoral fin of *Polypterus*. Previously, *in vitro* isolated muscle preparations have been widely used for the evaluation of muscle function (rats (Fletcher et al., 2020; Ganji et al., 2021); zebrafish (Sloboda et al., 2013); *Anolis* (Foster & Higham, 2016)). The isolated fin muscles will also be stretched to the extreme until they are torn to measure the limitation of the muscle length. If we could measure the cyclical muscle length change during walking, we would set up an *in vitro* muscle contractile test to measure muscle force and length change. It would allow us to change muscle stimulation pattern and length change independently and simultaneously to successfully acquire force-length and force-velocity curves as well as work loops for each muscle. We could even extend the protocols to test the extreme performance of the muscle tissue and compare how close swimming and walking motions are to the maximum performance of the muscle tissue. We would expect the zono muscle to work as a motor during the swing phase as we predict it facilitated swinging the fin away from the body trunk. We would expect the abductor to function as a strut during stance as it requires force and endurance when holding and stabilizing the fin on the ground.

We suggested that the pectoral fin muscles would need to contract faster to achieve the higher adduction velocity observed on land. Such rapid movement would require fast muscle contractions of short duration. Thus, white muscle fiber is likely used to increase the adduction speed during walking, which could be a driving force of the observed muscle fiber type transition after an extended period of walking (Du & Standen, 2017). For further investigation, we could perform a wavelet analysis on the EMG signals of the pectoral fin muscles to understand the relative activation of white and red muscle fibers. The wavelet analysis looks at the time and frequency of the intensity of the EMG signal (Tscharner, 2000) and allows us to isolate the EMG signals in a lower frequency and higher frequency range. As white muscle fiber and red muscle fiber are known as fast twitch and slow twitch muscle fiber, we could use the wavelet with high frequency, and low frequency as a proxy to look at white muscle, and red muscle fiber recruitment. Understanding the wavelet distribution would tell us whether there was a difference in which muscles are recruited in swimming compared with walking. If white fibers are recruited more often during walking, this could explain the switch to white muscle fibers seen in fish kept on the land.

References

Appelt, H.-J., Soares, J. M. C., & Duarte, J. A. R. (1992). Exercise, Muscle Damage and Fatigue. *Sports Medicine*, *13*(2), 108–115.

Batschelet, E. (1981). *Circular statistics in biology*. Academic press.

Betancur-R, R., Wiley, E. O., Arratia, G., Acero, A., Bailly, N., Miya, M., Lecointre, G., & Ortí, G. (2017). Phylogenetic classification of bony fishes. *BMC Evolutionary Biology*, *17*, 162. https://doi.org/10.1186/s12862-017-0958-3

Clack, J. A. (2012). *Gaining ground: the origin and evolution of tetrapods*. Indiana University Press.

Cuervo, R., Hernández-Martínez, R., Chimal-Monroy, J., Merchant-Larios, H., & Covarrubias, L. (2012). Full regeneration of the tribasal Polypterus fin. *Proceedings of the National Academy of Sciences of the United States of America*, *109*(10), 3838–3843. https://doi.org/10.1073/pnas.1006619109

Davidovits, P. (2013). Static Forces. In *Physics in Biology and Medicine* (pp. 1–21). Elsevier. https://doi.org/10.1016/B978-0-12-386513-7.00001-1

Del Coso, J., Gonzá lez-Millá, C., José Salinero, J., Abiá n-Vicé, J., Soriano, L., Garde, S., & Pé rez-Gonzá lez, B. (2012). Muscle Damage and Its Relationship with Muscle Fatigue During a Half-Iron Triathlon. *PLoS One*, *7*(8). https://doi.org/10.1371/journal.pone.0043280

Dhuper, M. (2018). *Understanding the functional morphology of the pectoral fin in Polypterus senegalus*. University of Ottawa.

Drucker, E. G., & Jensen, J. S. (1997). Kinematic and electromyographic analysis of steady pectoral fin swimming in the surfperches. *Journal of Experimental Biology*, *200*(12), 1709–1723. https://doi.org/10.1242/jeb.200.12.1709

Drucker, E. G., Walker, J. A., & Westneat, M. W. (2005). Mechanics of Pectoral Fin Swimming in Fishes. In R. E. S. George V Lauder (Ed.), *Fish Biomechanics* (Vol. 23, pp. 369–423). Academic Press. https://doi.org/10.1016/S1546-5098(05)23010-8

Du, T. Y., Larsson, H. C. E., & Standen, E. M. (2016). Observations of terrestrial locomotion in wild *Polypterus senegalus* from Lake Albert, Uganda. *African Journal of Aquatic Science*, *41*(1), 67–71. https://doi.org/10.2989/16085914.2015.1125337

Du, T. Y., & Standen, E. M. (2017). Phenotypic plasticity of muscle fiber type in the pectoral fins of *Polypterus senegalus* reared in a terrestrial environment. *Journal of Experimental Biology*, *220*(19), 3406–3410. https://doi.org/10.1242/jeb.162909

Du, T. Y., & Standen, E. M. (2020). Terrestrial acclimation and exercise lead to bone functional response in *Polypterus senegalu*s pectoral fins. *Journal of Experimental Biology*, *223*(11). https://doi.org/10.1242/jeb.217554

Fenwick, A. J., Wood, A. M., & Tanner, B. C. W. (2017). Effects of cross-bridge compliance on the

force-velocity relationship and muscle power output. *PLOS ONE*, *12*(12), e0190335. https://doi.org/10.1371/journal.pone.0190335

Foster, K. L., Dhuper, M., & Standen, E. M. (2018). Fin and body neuromuscular coordination changes during walking and swimming in *Polypterus senegalus*. *Journal of Experimental Biology*. https://doi.org/10.1242/jeb.168716

Garrett, J. (1996). Muscle strain injuries. *American Journal of Sports Medicine*, *24*(SUPPL.), 2–8. https://doi.org/10.1177/036354659602406s02

George R. McGhee. (2013). *When the Invasion of Land Failed: The Legacy of the Devonian Extinctions*. Columbia University Press. https://doi.org/10.7312/mcgh16056

Gordon, A. M., Huxley, A. F., & Julian, F. J. (1966). The variation in isometric tension with sarcomere length in vertebrate muscle fibres. *The Journal of Physiology*, *184*(1), 170–192. https://doi.org/10.1113/jphysiol.1966.sp007909

Graham, J. B., Wegner, N. C., Miller, L. A., Jew, C. J., Lai, N. C., Berquist, R. M., Frank, L. R., & Long, J. A. (2014). Spiracular air breathing in polypterid fishes and its implications for aerial respiration in stem tetrapods. *Nature Communications*, *5*(May 2013), 1–6. https://doi.org/10.1038/ncomms4022

Hedrick, T. L. (2008). Software techniques for two- and three-dimensional kinematic measurements of biological and biomimetic systems. *Bioinspiration & Biomimetics*, *3*(3), 034001. https://doi.org/10.1088/1748-3182/3/3/034001

Herbison, G. J., Jaweed, M. M., & Ditunno, J. F. (1982). Muscle fiber types. *Archives of Physical Medicine and Rehabilitation*, *63*(5), 227–230. http://www.ncbi.nlm.nih.gov/pubmed/6462127

Hunter, A. M., Galloway, S. D. R., Smith, I. J., Tallent, J., Ditroilo, M., Fairweather, M. M., & Howatson, G. (2012). Assessment of eccentric exercise-induced muscle damage of the elbow flexors by tensiomyography. *Journal of Electromyography and Kinesiology*, *22*(3), 334–341. https://doi.org/10.1016/j.jelekin.2012.01.009

Infantolino, B. W., Ellis, M. J., & Challis, J. H. (2010). Individual Sarcomere Lengths in Whole Muscle Fibers and Optimal Fiber Length Computation. *The Anatomical Record: Advances in Integrative Anatomy and Evolutionary Biology*, *293*(11), 1913–1919. https://doi.org/10.1002/ar.21239

Ivanova, N., Gugleva, V., Dobreva, M., Pehlivanov, I., Stefanov, S., & Andonova, V. (2016). Biological Propulsion Systems for Ships and Underwater Vehicles. In *Intech: Vol. i* (Issue tourism, p. 13). https://doi.org/10.5772/intechopen.82830.

Jayne, B. C., & Lauder, G. V. (1993). Red and white muscle activity and kinematics of the escape response of the bluegill sunfish during swimming. *Journal of Comparative Physiology A*, *173*(4), 495–508. https://doi.org/10.1007/BF00193522

Jayne, B. C., & Lauder, G. V. (1994). How swimming fish use slow and fast muscle fibers:

implications for models of vertebrate muscle recruitment. *Journal of Comparative Physiology A*, *175*(1), 123–131. https://doi.org/10.1007/BF00217443

Jerrold H. Zar. (1999). *Biostatistical analysis*. Pearson.

Landler, L., Ruxton, G. D., & Malkemper, E. P. (2019). The Hermans-Rasson test as a powerful alternative to the Rayleigh test for circular statistics in biology. *BMC Ecology*, *19*(1), 4–11. https://doi.org/10.1186/s12898-019-0246-8

Mansfield, P. J., & Neumann, D. A. (2019). Structure and Function of Skeletal Muscle. In *Essentials of Kinesiology for the Physical Therapist Assistant* (pp. 34–49). Elsevier. https://doi.org/10.1016/B978-0-323-54498-6.00003-5

Miyake, T., Kumamoto, M., Iwata, M., Sato, R., Okabe, M., Koie, H., Kumai, N., Fujii, K., Matsuzaki, K., Nakamura, C., Yamauchi, S., Yoshida, K., Yoshimura, K., Komoda, A., Uyeno, T., & Abe, Y. (2016). The pectoral fin muscles of the coelacanth Latimeria chalumnae: Functional and evolutionary implications for the fin-to-limb transition and subsequent evolution of tetrapods. *Anatomical Record*, *299*(9), 1203–1223. https://doi.org/10.1002/ar.23392

Morgan, D. L., Allen, D. G., & Early, D. G. A. (1999). invited review Early events in stretch-induced muscle damage. In *J. Appl. Physiol* (Vol. 87, Issue 6). http://www.jap.org

Pette, D. (1998). Training effects on the contractile apparatus. *Acta Physiologica Scandinavica*, *162*(3), 367–376. https://doi.org/10.1046/j.1365-201X.1998.0296e.x

Radák, Z. (2018). Skeletal Muscle, Function, and Muscle Fiber Types. In *The Physiology of Physical Training* (pp. 15–31). Elsevier. https://doi.org/10.1016/b978-0-12-815137-2.00002-4

Rassier, D., MacIntosh, B., & Herzog, W. (1998). Length dependence of active force production in skeletal muscle. *Vascular Surgery*, *32*(3), 245–247. https://doi.org/10.1177/153857449803200307

Roberts, T. J., & Gabaldón, A. M. (2008). Interpreting muscle function from EMG: Lessons learned from direct measurements of muscle force. *Integrative and Comparative Biology*, *48*(2), 312–320. https://doi.org/10.1093/icb/icn056

Schiaffino, S., & Reggiani, C. (2011). Fiber types in Mammalian skeletal muscles. *Physiological Reviews*, *91*(4), 1447–1531. https://doi.org/10.1152/physrev.00031.2010

Schneider, I., & Shubin, N. H. (2013). The origin of the tetrapod limb: from expeditions to enhancers. *Trends in Genetics*, *29*(7), 419–426. https://doi.org/10.1016/j.tig.2013.01.012

Sfakiotakis, M., Lane, D. M., & Davies, J. B. C. (1999). Review of fish swimming moeds for aquatic locomotion. *Journal of Oceanic Engineering*, *24*(2), 237–252. file:///Z:/Commercial/Current_Projects/14001/Research_Literature/Fish_Swimming_Techniques.pdf

Sharon Plowman, Denise L Smith. (2007). Anaerobic Metabolism during Exercise. In *Sports-*

Specific Rehabilitation (pp. 39–63). Elsevier. https://doi.org/10.1016/B978-044306642-9.50006-X

Shekarchizadeh, P., Enayat, M., & Karimian, J. (2018). The Effect of Branched Chain Amino Acids Supplementation (BCAA) on Muscle Damage and the Indicators of Fatigue in Soccer Players. *Atherosclerosis Supplements*, *32*(2018), 135–136. https://doi.org/10.1016/j.atherosclerosissup.2018.04.417

Standen, E. M., Du, T. Y., Laroche, P., & Larsson, H. C. E. (2016). Locomotor flexibility of *Polypterus senegalus* across various aquatic and terrestrial substrates. *Zoology*, *119*(5), 447–454. https://doi.org/10.1016/j.zool.2016.05.001

Standen, E. M., Du, T. Y., & Larsson, H. C. E. (2014). Developmental plasticity and the origin of tetrapods. *Nature*, *513*(7516), 54–58. https://doi.org/10.1038/nature13708

Suzuki, D., Brandley, M. C., & Tokita, M. (2010). The mitochondrial phylogeny of an ancient lineage of ray-finned fishes (Polypteridae) with implications for the evolution of body elongation, pelvic fin loss, and craniofacial morphology in Osteichthyes (BMC Evolutionary Biology (2010) 10 (21)). *BMC Evolutionary Biology*, *10*(1), 1–12. https://doi.org/10.1186/1471-2148-10-209

Tscharner, V. Von. (2000). Intensity analysis in time-frequency space of surface myoelectric signals by wavelets of specified resolution. *Journal of Electromyography and Kinesiology*, *10*(6), 433–445.

Vøllestad, N. K. (1997). Measurement of human muscle fatigue. *Journal of Neuroscience Methods*, *74*(2), 219–227. https://doi.org/10.1016/S0165-0270(97)02251-6

Wilhelm, B. C., Du, T. Y., Standen, E. M., & Larsson, H. C. E. (2015). Polypterus and the evolution of fish pectoral musculature. *Journal of Anatomy*. https://doi.org/10.1111/joa.12302

Wilson, J. M., Loenneke, J. P., Jo, E., Wilson, G. J., Zourdos, M. C., & Jeong-Su Kim. (2012). The Effects of Endurance, Strength, and Power Training on Muscle Fiber Type Shifting. *Journal of Strength and Conditioning Research*, *26*(6), 1724–1729.

Appendix: Supplementary tables and figures

Tables

Appendix Table 1: Results of mixed-model ANOVAs of supplementary kinematic variables between behaviours

Variables	Behaviour		F-value (d.f.)

	swim	walk	ANOVA p-value	
Nose swing distance ± s.e.m. (mm)	-	152.1 ± 6.41	-	-
Fin swing distance ± s.e.m. (mm)	34.96 ± 13.0	105.4 ± 11.9	0.0096*	16.60776(1,5)
Tail swing distance ± s.e.m. (mm)	120.1 ± 31.1	404.6 ± 27.0	<0.001*	80.80716(1,5)
Movement speed ± s.e.m. (mm/s)	75.65 ± 17.4	76.78 ± 16.4	0.9520	0.003999(1,5)

Each kinematic variable is compared between swimming and walking. Each trial is nested in the corresponding fish, and individual fish is coded as a random factor in the models. Asterisks represent for significant differences. Numerator and denominator d.f. (degree of freedom) are given in parentheses after F-values.

Appendix Table 2: Comparison of EMG variable changes from swimming to walking based on 95% CI of the estimated mean difference

contrasts	Fin variables	Fin muscles	Lower CI	Upper CI	Significantly different from
Swim - walk	**Activation duration**	Zono	-0.367	-0.164	
		abductor	-0.243	-0.0430	adductor
		Coraco	-0.233	-0.0323	adductor
		adductor	-0.488	-0.286	Abductor, coraco
	THRIA (% activation duration)	Zono	-0.1251	0.03511	
		abductor	-0.1680	-0.00607	
		Coraco	-0.0602	0.10284	
		adductor	-0.1331	0.02896	
	RIA (% maximum RIA)	Zono	-0.944	-0.3452	
		abductor	-0.856	-0.2597	
		Coraco	-0.906	-0.3079	
		adductor	-0.507	0.0917	
	Max Amp (% maximum burst amplitude)	Zono	-279	-84.4	
		abductor	-308	-115.6	
		Coraco	-280	-87.9	
		adductor	-213	-17.9	
		Zono	-0.1847	0.126	adductor

	Duty Factor (% activation duration)	abductor	-0.0847	0.22	adductor
		Coraco	-0.954	0.218	adductor
		adductor	-0.5513	-0.242	All other muscles
contrasts	**Body variables**	**Body position**	**Lower CI**	**Upper CI**	**Significantly different from**
Swim - walk	**Activation duration**	Body 5	-0.0146	0.16083	
		Body 6	-0.1818	0.00959	
		Body 7	-0.1478	0.04343	
		Body 8	-0.1566	0.01891	
	THRIA (% activation duration)	Body 5	-0.0921	0.0445	
		Body 6	-0.1749	-0.0218	
		Body 7	-0.0545	0.0795	(8)
		Body 8	-0.1910	-0.0578	(7)
	RIA (% maximum RIA)	Body 5	-71.9	-30.53	
		Body 6	-68.5	-27.15	(8)
		Body 7	-37.2	4.17	(8)
		Body 8	-110.2	-68.88	(6), (7)
	Max Amp (% maximum burst amplitude)	Body 5	-562	-297	
		Body 6	-510	-245	
		Body 7	-271	-5.98	(8)
		Body 8	-641	-376	(7)
	Duty Factor (% activation duration)	Body 5	0.0645	0.4323	
		Body 6	-0.2927	0.1118	
		Body 7	-0.2544	0.1001	
		Body 8	-0.2621	0.0923	

95% confidence intervals (95% CIs) are calculated based on the linear mixed effect models along with the marginal means of the EMG variable change. When one set of CIs do not overlap with another set, the change in difference between two fin muscles/body positions are significantly different.

Figures

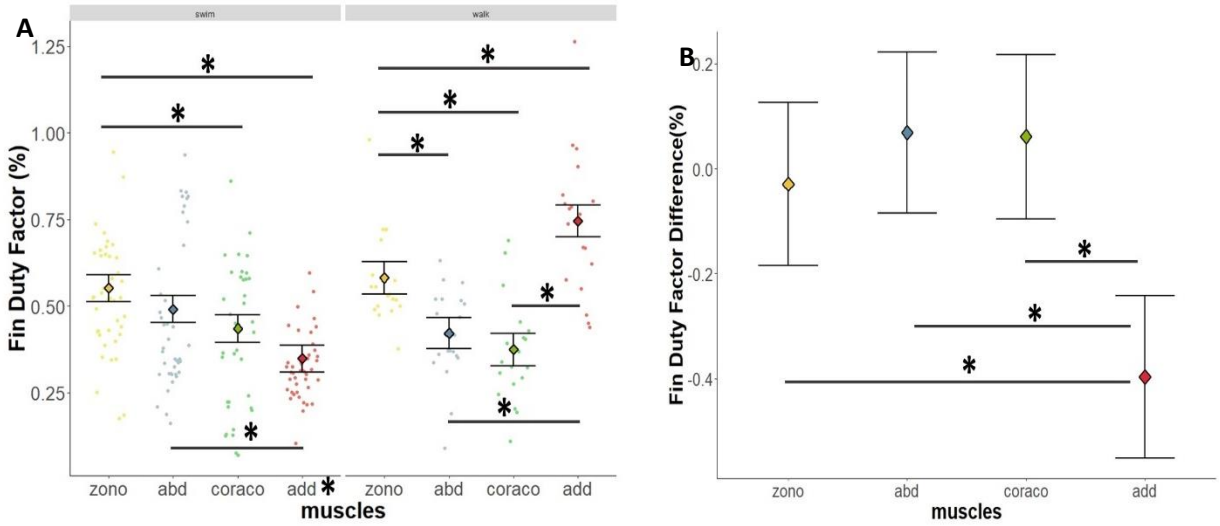

Appendix Figure 1: Results of duty factor in pectoral fin muscles. (A) duty factor of each muscle was expressed in percentage of activation duration within swimming (at the left), and walking (at the right). Values are presented as emmean ± s.e.m. Individual data are the paler shaded dots behind the emmean. Asterisks with thin bars indicate significant differences across muscle within each behaviour **(**reported in **Table 3.1)**. Asterisks besides muscles on the x-axis label indicate significant differences between swimming and walking for the corresponding muscle (P-values reported in **Table 3.2**). **(B)** The change of fin duty factor difference from swimming to walking for each muscle was presented as the emmean difference ± 95% CI. Asterisks with thin bars indicate significant differences in the change from swimming to walking among muscles (**Appendix Table 2**).

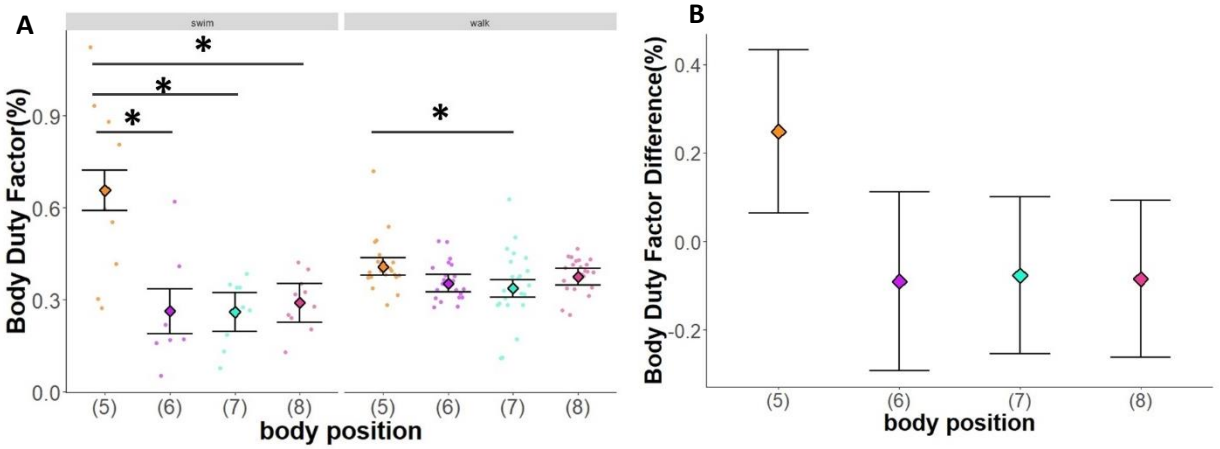

Appendix Figure 2: Results of duty factor in body positions. (A) duty factor of each muscle was expressed in percentage of activation duration within swimming (at the left), and walking (at the right). Values are presented as emmean ± s.e.m. Individual data are the paler shaded dots behind the emmean. Asterisks with thin bars indicate significant differences across muscle within each behaviour **(**reported in **Table 3.1)**. Asterisks besides muscles on the x-axis label indicate significant differences between swimming and walking for the corresponding muscle (P-values

reported in **Table 3.2**). **(B)** The change of fin duty factor difference from swimming to walking for each muscle was presented as the emmean difference ± 95% CI. Asterisks with thin bars indicate significant differences in the change from swimming to walking among muscles (**Appendix Table 2**).

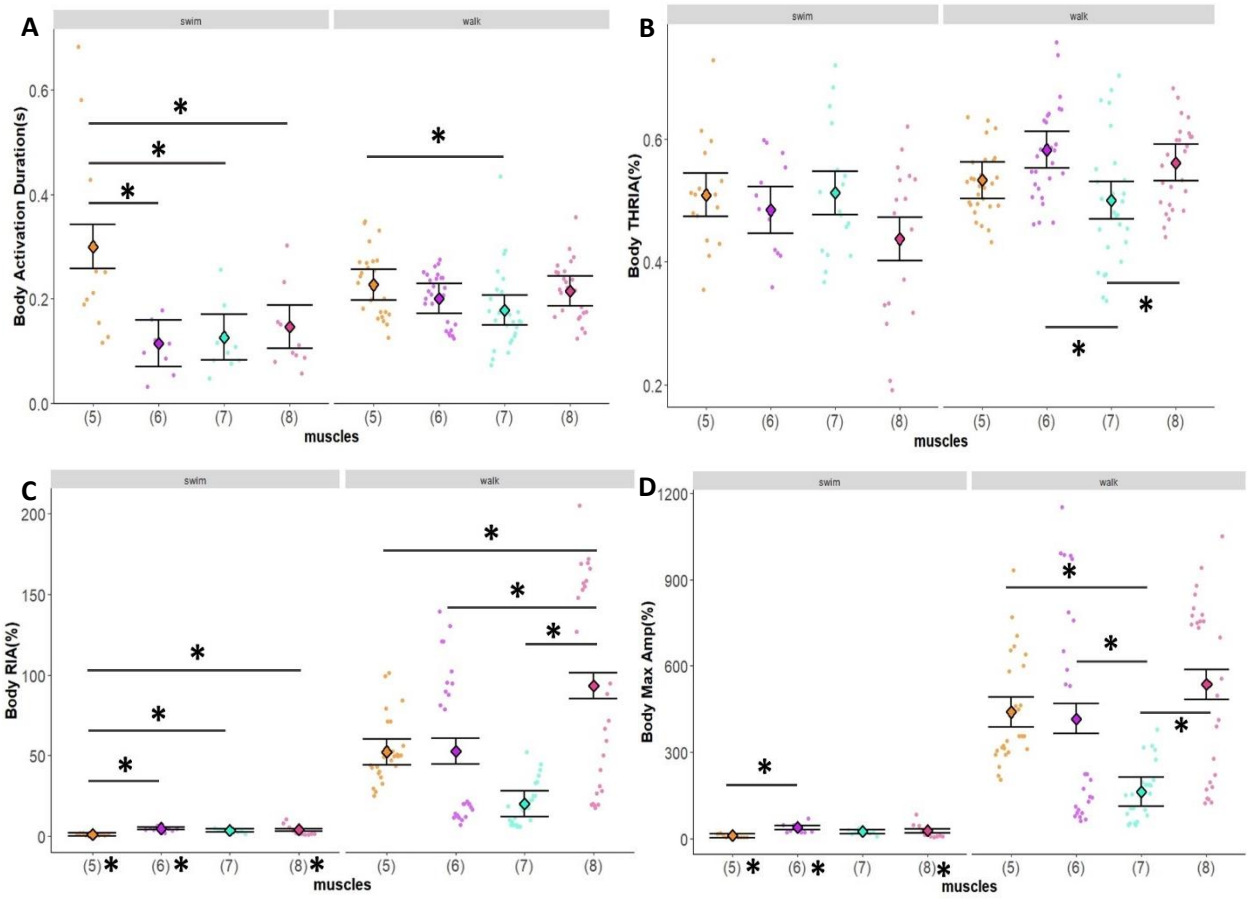

Appendix Figure 3: Differences in muscle activity of body position magnitude variables. (A) Activation duration is expressed as the time in second of how long a muscle turns on. (B) Time to half RIA (THRIA) is expressed as a percentage of activation duration. (C) Maximum amplitude of each muscle burst is expressed as a percentage of the maximum amplitude observed in a reference trial with steady motion for each individual. (D) Rectified integrated area (RIA) of each muscle burst expressed as a percentage of maximum reference burst RIA. All of the values are presented as emmean ± s.e.m. Individual data are the paler shaded dots behind the emmean. The order of the muscles listed in the graph corresponds to electrode implantation locations (as in Figure 2.1). Colours correspond to the electrode placement of zono, abductor, coraco, and adductor in Figure 2.1. Asterisks with thin bars indicate significant differences between muscles within each behaviour (swimming and walking). Significances are shown in Table 3.1. Asterisks besides muscles on the x-axis label indicate significant differences between swimming and walking for the corresponding muscle (P-values reported in Table 3.2).

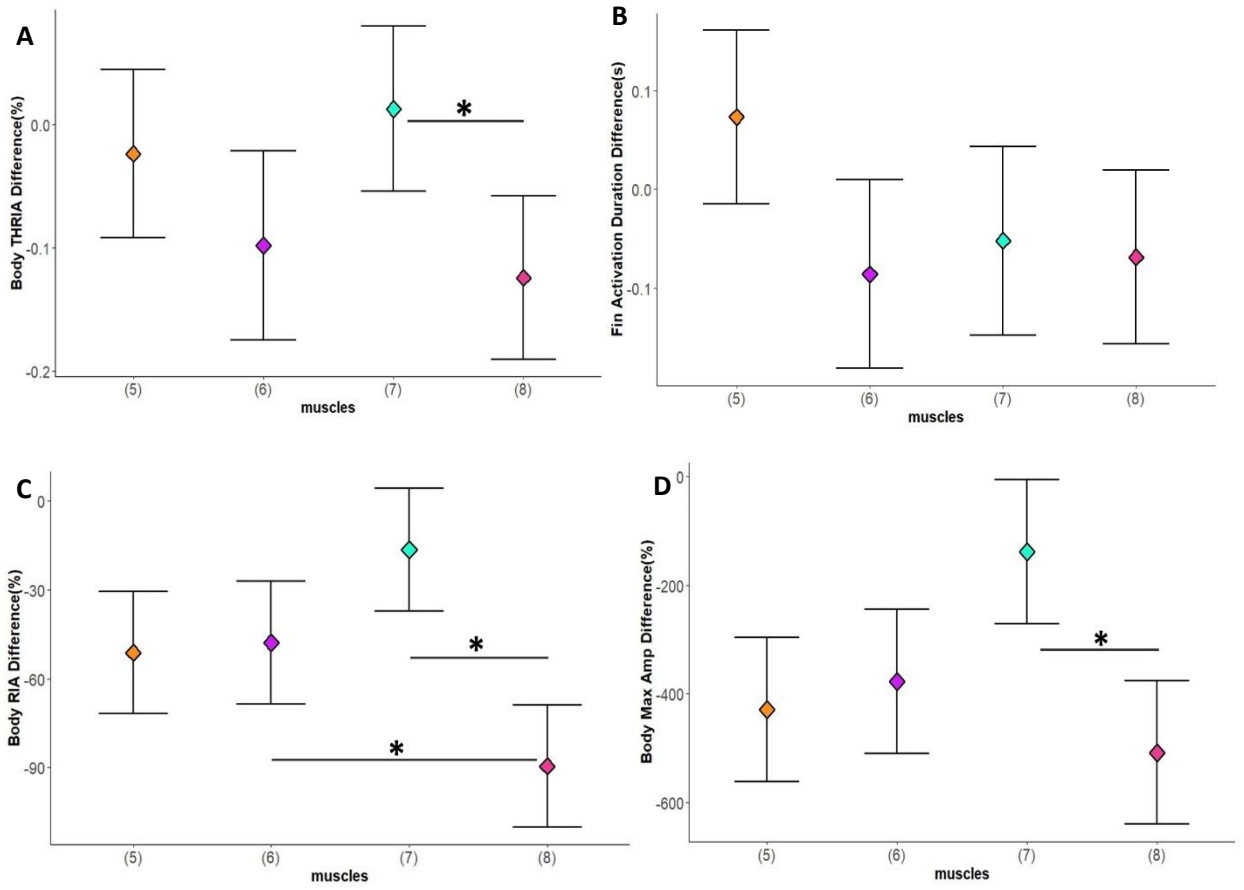

Appendix Figure 4: Differences between swimming and walking for muscle activity of body position magnitude variables. The change of (A) activation duration, (B) THRIA, (C) maximum amplitude, and (D) burst RIA from swimming to walking is listed in the same order as the corresponding variables in **Figure 2.9 (A)** to **(D)**. All of the values are presented as the contrast of emmean between swim and walk ± 95% CI (Emmean = estimated marginal means; 95% CI = 95% confidence interval). The order and colour codes of the muscles listed in the graphs corresponds to electrode implantation locations (as in **Figure 2.1;** zono=yellow, abductor=blue, coraco=green, and add=red). Asterisks with thin bars indicate significant differences in the change from swimming to walking among muscles (**Appendix Table 2**).

A

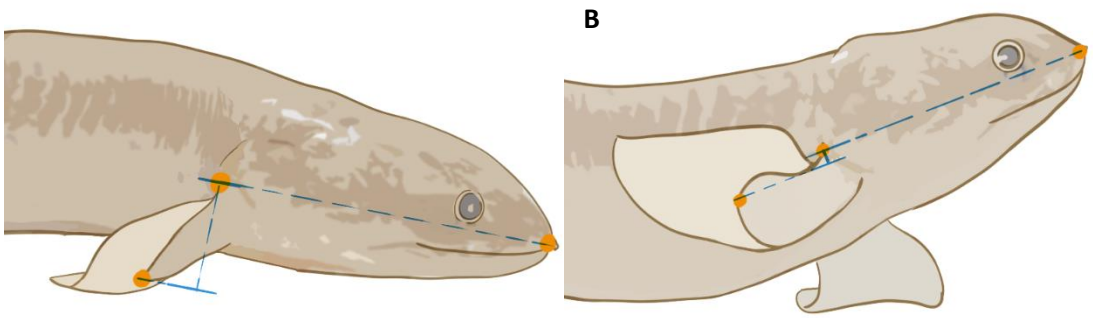

Appendix Figure 5: Illustration of a walking fish at maximum elevation (A) and minimum elevation (B). The fin elevation (as described in Figure 2.5 E) at the maximum and minimum is presented from the lateral view. The illustration was done by tracing on the specific frame of a trial when the fin reached maximum elevation (A, Figure 2.5 G) and minimum elevation (B, Figure 2.5 H).

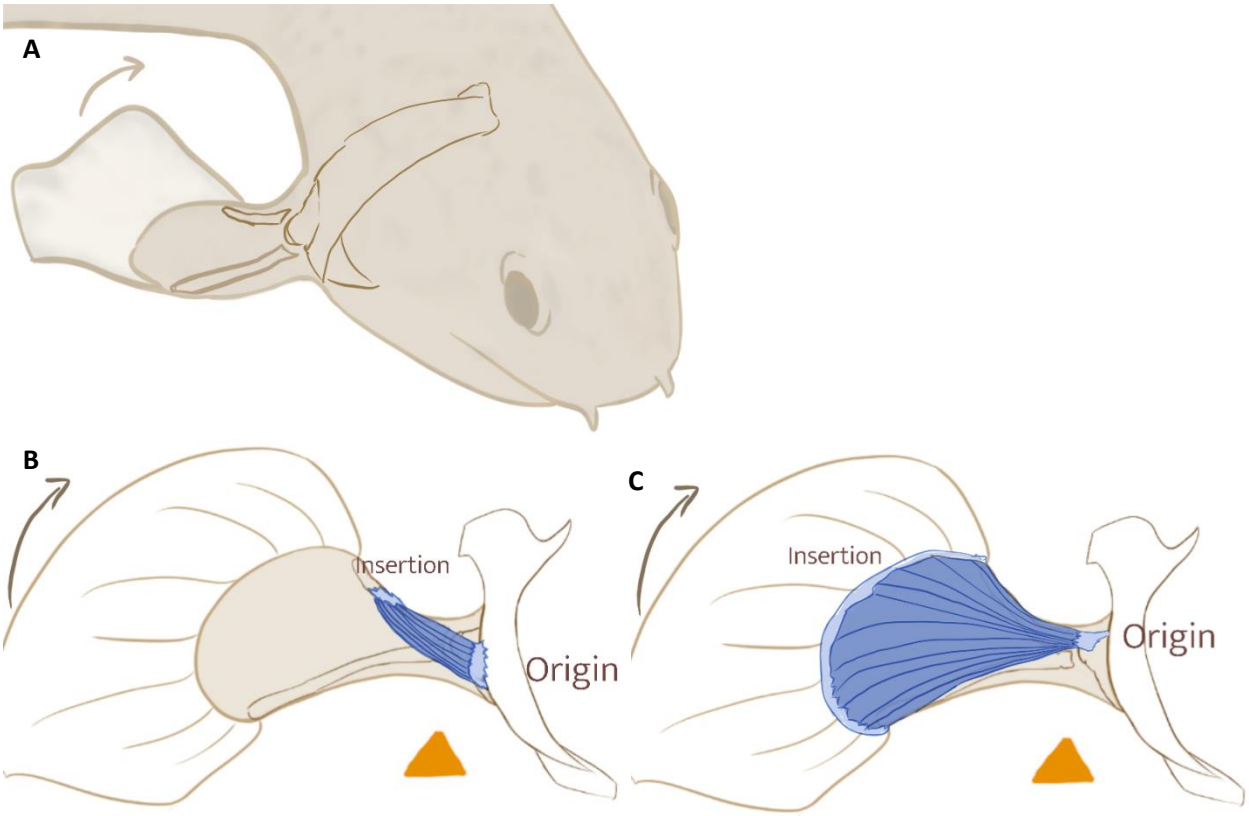

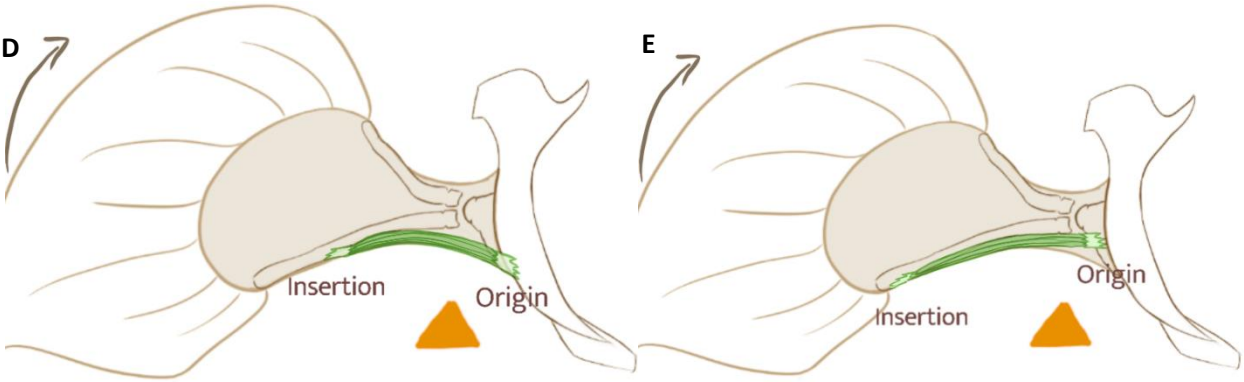

Appendix Figure 5: Schematic pectoral fin musculature of two abductor and coraco muscles. (A) Placement of the pectoral girdle and fin bones in a walking fish. The shorter muscle, abductor superficialis (B), and the longer muscle, abductor profundus (C) are coloured in blue. The shorter muscle, coraco II (D), and the longer muscle, coraco I (E) are coloured in green. The muscles are presented from the medial side of the fin. Insertion and origin of each muscle are indicated in the graphs. The anatomy is consistent with **Figure 2.1** and based on the study by Wilhelm *et al.* (2015).

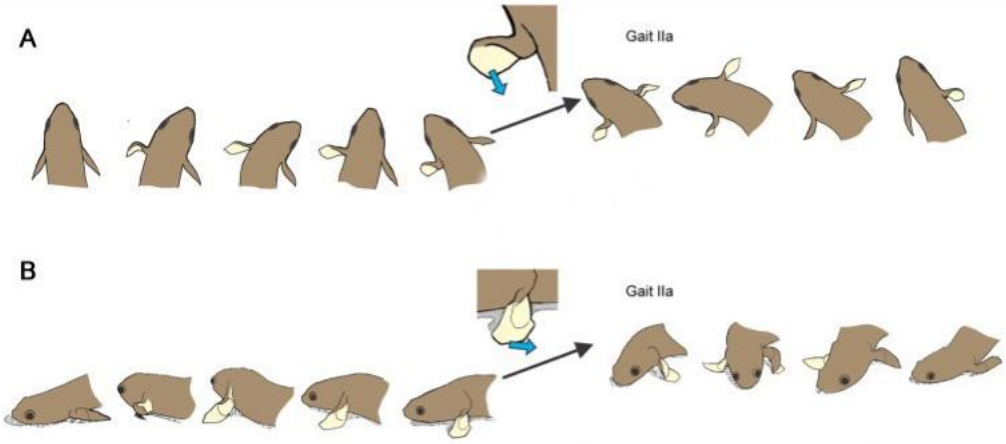

Appendix Figure 6: Illustration of walking pattern, gait IIa of the pectoral fin. (A) and (B) are illustrated in dorsal view and lateral view. During gait IIa the fin puts its lateral side throughout stance phase and the fin is slid along the ground, adducted toward the body and then supinated and lifted off the ground. The picture is edited and borrowed from Standen et al. (2016).